

RATE-OPTIMAL HIGHER-ORDER ADAPTIVE CONFORMING FEM FOR BIHARMONIC EIGENVALUE PROBLEMS ON POLYGONAL DOMAINS

CARSTEN CARSTENSEN AND BENEDIKT GRÄSSLE

ABSTRACT. The a posteriori error analysis of the classical Argyris finite element methods dates back to 1996, while the optimal convergence rates of associated adaptive finite element schemes are established only very recently in 2021. It took a long time to realise the necessity of an extension of the classical finite element spaces to make them hierarchical. This paper establishes the novel adaptive schemes for the biharmonic eigenvalue problems and provides a mathematical proof of optimal convergence rates towards a simple eigenvalue and numerical evidence thereof. This makes the suggested algorithm highly competitive and clearly justifies the higher computational and implementational costs compared to low-order nonconforming schemes. The numerical experiments provide overwhelming evidence that higher polynomial degrees pay off with higher convergence rates and underline that adaptive mesh-refining is mandatory. Five computational benchmarks display accurate reference eigenvalues up to 30 digits.

1. INTRODUCTION

The conforming Argyris finite element method (FEM) of polynomial order $p \geq 5$ allows for an optimally convergent adaptive scheme that provides guaranteed upper eigenvalue bounds by the min-max principle.

1.1. State of the art. The conforming discretisation of the fourth-order problems with C^1 conforming elements like the Hsieh-Clough-Tocher, Bell, or Argyris is textbooks material [Cia02]. The lowest-order Argyris element consists of quintic polynomials and was also described by Bell [Bel68, Bel69], Bosshard [Bos68], Visser [Vis68], Withum [Wit66], and Argyris, Fried, Scharpf [AFS68]. The a posteriori error control for the Argyris FEM is known for more than two decades and even included in the first book [Ver96] on a posteriori error analysis. But optimal convergence rates of the associated adaptive algorithm were established only recently for a hierarchical Argyris FEM [CH21] for the plain discretisation. The higher convergence rates of the Argyris FEM are rarely visible even in simple computational benchmarks with the biharmonic equation and a right-hand side in L^2 in a polygonal bounded Lipschitz domain Ω . In contrast, the non-conforming adaptive Morley FEM is known to be optimal for at least one decade [HSX12, CGH14] with an implementation in only 30 lines of MATLAB.

1.2. Overview. This paper considers conforming discretisations of eigenvalue problems with hierarchical subspaces $V(\mathcal{T}_0) \subset V(\mathcal{T}_1) \subset \dots \subset V$ over a nested sequence of triangulations $(\mathcal{T}_\ell)_\ell$ generated by the adaptive algorithm AFEM of Figure 1. The adaptive algorithm refines towards regions of the mesh with a high contribution to the error estimator η and enables optimal convergence rates. The key difficulty in the proof of optimal convergence rates for AFEM in the present setting with a hierarchical and conforming method is the discrete reliability. The hierarchical structure of the resulting hierarchical Argyris FEM introduced in [CH21] enables guaranteed optimal convergence rates for the source problem [CH21, Grä22]. This paper establishes the novel adaptive schemes for biharmonic eigenvalue problems and provides a mathematical proof of optimal convergence rates towards a simple eigenvalue in Section 2. The key lemma provides a uniformly improved L^2 error control relative to the H^2 energy norm of two discrete eigenvector approximations on two different but nested triangulations and associated discrete spaces. The framework of elliptic eigenvalue approximations in [CFPP14, Sub. 10.3] is rewritten and improved. Section 3 establishes the four axioms (A1)–(A4) for optimal convergence rates of the hierarchical Argyris eigenvalue solver. This asserts the high convergence rates of the p -th order scheme (for $p \geq 5$) in many practical examples.

The implementation follows [CH21, Grä22] and allows the adaptive computation of all kinds of eigenvalue problems related to the bi-Laplace operator. The first example is the computation of the first reference eigenvalues in more than 30 digits in Subsection 4.2 for the square and the L-shaped domain in

This work has been supported by the *Deutsche Forschungsgemeinschaft* (DFG) in the Priority Program 1748 *Reliable simulation techniques in solid mechanics: Development of non-standard discretization methods, mechanical and mathematical analysis* under the project CA 151/22-2. The second author is also supported by the DFG under Germany's Excellence Strategy – The Berlin Mathematics Research Center MATH+ (EXC-2046/1, project ID: 390685689).

AFEM.
Input: Initial triangulation \mathcal{T}_0 , $0 < \theta < 1$, and eigenpair number $j \in \mathbb{N}$
for $\ell = 0, 1, 2, \dots$ **do**
 Compute the j -th discrete eigenpair $(\lambda_\ell, u_\ell) \in \mathbb{R}_+ \times V(\mathcal{T}_\ell)$ with (2) on $\mathcal{T} \equiv \mathcal{T}_\ell$
 Compute $\eta_\ell(T) := \eta(T)$ from (3) for all $T \in \mathcal{T} \equiv \mathcal{T}_\ell$
 Mark subset $\mathcal{M}_\ell \subset \mathcal{T}_\ell$ with $\theta \eta_\ell^2(\mathcal{T}) \leq \eta_\ell^2(\mathcal{M}_\ell) := \sum_{T \in \mathcal{M}_\ell} \eta_\ell^2(T)$ and minimal cardinality $|\mathcal{M}_\ell| \geq 1$
 Compute smallest NVB refinement $\mathcal{T}_{\ell+1}$ of \mathcal{T}_ℓ with $\mathcal{M}_\ell \subseteq \mathcal{T}_\ell \setminus \mathcal{T}_{\ell+1}$ **od**
Output: Sequence of triangulations \mathcal{T}_ℓ , error estimators η_ℓ , and eigenpairs $(\lambda_\ell, u_\ell) \in \mathbb{R}_+ \times V(\mathcal{T}_\ell)$

FIGURE 1. Adaptive Argyris finite element scheme AFEM

Subsection 4.3 with clamped boundary conditions. Isospectral domains are well established for the Laplacian and Subsection 4.4 investigates this question for the bi-Laplacian: There exist isospectral domains for the simply-supported plate but those domains have a different spectrum under clamped boundary conditions. A more practical example in Subsection 4.5 encounters the computational engineering of a vibrating plate with clamped and free boundary conditions. The final example in Subsection 4.6 concerns the computation of optimal constants in basic estimates of numerical analysis: Two Friedrichs inequalities and interpolation error estimates illustrate that all kind of boundary conditions can be included. Optimal convergence rates are visible for all examples and thereby clearly justify the higher computational and implementational costs compared to low-order nonconforming schemes: The numerical experiments provide overwhelming evidence that higher polynomial degrees pay off with higher convergence rates and underline that adaptive mesh-refining is mandatory.

1.3. Biharmonic eigenvalue problem and discretisation. Given a bounded Lipschitz domain $\Omega \subset \mathbb{R}^2$ with polygonal boundary $\partial\Omega$ and outer unit normal ν , the vector space of admissible functions

$$V := \{v \in H^2(\Omega) : v|_{\partial\Omega} \equiv 0 \equiv \partial_\nu v|_{\partial\Omega}\}$$

of continuous functions with square integrable Lebesgue partial derivatives up to second order and clamped boundary conditions. The Hessian $Dv \in L^2(\Omega)^{2 \times 2}$ defines the energy scalar product

$$a(\bullet, \bullet) := (D^2\bullet, D^2\bullet)_{L^2(\Omega)}$$

and with the L^2 scalar product

$$b(\bullet, \bullet) := (\bullet, \bullet)_{L^2(\Omega)}.$$

The weak formulation of the biharmonic eigenvalue problems seeks an eigenpair $(\lambda, u) \in \mathbb{R}_+ \times V \setminus \{0\}$ with $b(u, u) = 1$ and

$$(1) \quad a(u, v) = \lambda b(u, v) \quad \text{for all } v \in V.$$

Throughout this paper, let \mathcal{T} denote a regular triangulation of the domain Ω into compact (non-degenerate) triangles. The conforming finite element method (FEM) for the discretisation of (1) requires C^1 conforming elements to define the discrete test space $V(\mathcal{T})$ and seeks a discrete eigenpair $(\lambda_h, u_h) \in \mathbb{R}_+ \times V(\mathcal{T}) \setminus \{0\}$ with $b(u_h, u_h) = 1$ and

$$(2) \quad a(u_h, v_h) = \lambda_h b(u_h, v_h) \quad \text{for all } v_h \in V(\mathcal{T}).$$

The discrete eigenvalue problem (2) provides $N := \dim V(\mathcal{T})$ discrete eigenvalues

$$0 < \lambda_h(1) \leq \lambda_h(2) \leq \dots \leq \lambda_h(N) < \infty =: \lambda_h(N+1) =: \lambda_h(N+2) =: \dots.$$

1.4. Explicit residual-based a posteriori error estimator. The local contribution $\eta(T)$ of a triangle $T \in \mathcal{T}$ with area $|T| > 0$ and boundary ∂T is the square root of

$$(3) \quad \eta^2(T) = |T|^2 \|\lambda_h u_h - \Delta^2 u_h\|_{L^2(T)}^2 + |T|^{1/2} \|[\partial_{\nu\nu}^2 u_h]_E\|_{L^2(\partial T \cap \Omega)}^2 + |T|^{3/2} \|[\partial_\nu \Delta u_h]_E\|_{L^2(\partial T \cap \Omega)}^2.$$

The jumps $[\bullet]_E$ apply only along the parts $\partial T \cap \Omega$ of the skeleton inside the domain across an interior edge E and only to the derivatives of the piecewise polynomial discrete solution u_h ; Δ is the Laplacian and $\partial_\nu \Delta$ is its normal derivative.

1.5. Adaptive algorithm AFEM. The adaptive algorithm depicted in Figure 1 is based on the local refinement indicators (3) in a standard (Dörfler) marking procedure and a mesh-refining by newest-vertex bisection (NVB) [Ste08]. The NVB defines a set \mathbb{T} of uniformly shape-regular admissible triangulations.

The theoretical result of this paper is the optimal convergence of the adaptive algorithm AFEM for sufficiently fine triangulations with mesh-size $h_{\max} \leq \delta$ in $\mathbb{T}(\delta)$ and a sufficiently small bulk parameter θ .

Theorem 1.1 (optimal rates). *If $\lambda = \lambda_j$ is a simple eigenvalue, then there exists $0 < \delta, \Theta$, that exclusively depend on Ω and the shape-regularity of \mathbb{T} such that for any $0 < s < \infty$ the output $(\mathcal{T}_\ell)_\ell$ and $(\eta_\ell)_\ell$ of the adaptive algorithm AFEM with bulk parameter $0 < \theta < \Theta$ and initial triangulation $\mathcal{T}_0 \in \mathbb{T}(\delta)$ satisfies*

$$(4) \quad \sup_{\ell \in \mathbb{N}_0} (1 + |\mathcal{T}_\ell| - |\mathcal{T}_0|)^s \eta_\ell \approx \sup_{N \in \mathbb{N}_0} (1 + N)^s \min \eta(\mathbb{T}(N)).$$

The proof of Theorem 1.1 concludes in Subsection 3.6.

1.6. Outline. The remaining parts of the paper are organised as follows. Section 2 establishes a rather abstract framework for symmetric elliptic eigenvalue problems with Rayleigh quotient in a Gelfand or evolution triple and provides a key lemma for the discrete stability on discrete eigenpairs in a 2-level situation. This enables a 2-level a posteriori error estimation in Lemma 2.2. Those results are essentially known although the framework of [CFPP14, Sub. 10.3] utilises different error terms. Section 3 applies those preliminary results and derives stability (A1), reduction (A2), discrete reliability (A3), and quasi-orthogonality (A4) for an extended Argyris finite element scheme of degree $p \geq 5$. This implies optimal convergence rates (4) as the main theoretical result of this paper. Numerical examples in Section 4 provide striking evidence of the recovered higher convergence rates that lead to a rehabilitation of the Argyris finite elements: The higher implementation costs clearly pay off. It underlines that adaptivity is mandatory and leads to highly accurate results. Five computational benchmarks provide reference values for the first 10 eigenvalues in high accuracy.

1.7. General notation. Standard notation for Lebesgue and Sobolev spaces and their norms applies throughout this paper; let $H^s(K)$ abbreviate $H^s(\text{int}(K))$ for a (compact) triangle K and any $s \in \mathbb{R}$. Let $P_k(M)$ denote the spaces of polynomials up to degree $k \in \mathbb{N}_0$ on some triangle or edge M with diameter $h_M \in P_0(M)$. The associated L^2 projection $\Pi_{M,k} : L^2(K) \rightarrow P_k(M)$ is defined by the L^2 orthogonality $(1 - \Pi_{M,k})v \perp P_k(M)$ for all $v \in L^2(M)$. Let

$$P_k(\mathcal{T}) := \{p \in L^\infty(\Omega) : p|_T \in P_k(T) \text{ for all } T \in \mathcal{T}\}$$

denote the space of piecewise polynomials with respect to a regular triangulation \mathcal{T} of Ω .

2. FOUNDATIONS OF A POSTERIORI ANALYSIS FOR CONFORMING EVP

This section verifies the axioms of adaptivity of an abstract conforming and hierarchical discretisation of a symmetric elliptic eigenvalue problem based on the two scalar products $a(\bullet, \bullet)$ and $b(\bullet, \bullet)$.

2.1. Abstract elliptic eigenvalue problem. This subsection considers an evolution or Gelfand triple (V, H, V^*) with the separable infinite-dimensional Hilbert spaces (V, a) and (H, b) and their induced norms $\|\bullet\| := a(\bullet, \bullet)^{1/2}$ and $\|\bullet\| := b(\bullet, \bullet)^{1/2}$ with the compact and dense embeddings

$$(5) \quad V \xhookrightarrow{c} H \equiv H^* \xhookrightarrow{c} V^*.$$

The abstract eigenvalue problem (EVP) seeks an eigenpair $(\lambda, u) \in \mathbb{R}_+ \times V$ with $\|u\| = 1$ and

$$(EVP) \quad a(u, v) = \lambda b(u, v) \quad \text{for all } v \in V.$$

The well-established spectral theory for the associated compact operators (from the compact and dense embeddings in (5)) provides that the countable eigenvalues to (EVP) have the only accumulation point at infinity and, counting their multiplicities, can be enumerated monotonously

$$0 < \lambda_1 \leq \lambda_2 \leq \lambda_3 \leq \dots \leq \lim_{j \rightarrow \infty} \lambda_j = \infty.$$

The finite dimension $m(j) \in \mathbb{N}$ of the subordinated eigenspaces $E(\lambda_j) = \{u \in V : a(u, \bullet) = \lambda_j b(u, \bullet)\}$ is equal to the multiplicity $m(j) \geq 1$ of λ_j in the enumeration, i.e., $\lambda_k < \lambda_{k+1} = \dots = \lambda_j = \dots = \lambda_{k+m(j)} < \lambda_{k+m(j)+1}$ for each $j \in \{k+1, \dots, k+m(j)\}$ and $k \in \mathbb{N}_0$ with $\lambda_0 := 0$. Moreover, the corresponding eigenvectors $\phi_1, \phi_2, \dots \in V$ are pairwise b -orthonormal as well as a -orthogonal,

$$a(\phi_j, \psi) = \lambda_j b(\phi_j, \psi) \quad \text{for all } \psi \in V, \quad a(\phi_j, \phi_k) = \lambda_j \delta_{jk}, \quad \text{and} \quad b(\phi_j, \phi_k) = \delta_{jk} \quad \text{for all } j, k \in \mathbb{N}$$

with the Kronecker delta δ_{jk} . We refer to textbooks [Bre11, Rud91, Yos95, Zei92] for the functional analysis and the aforementioned facts.

In the biharmonic example at hand for a polygonal bounded Lipschitz domain $\Omega \subset \mathbb{R}^2$, the inner products read

$$a(u, v) := \int_{\Omega} D^2 u : D^2 v \, dx \quad \text{and} \quad b(u, v) := \int_{\Omega} uv \, dx$$

for u, v in $V := H_0^2(\Omega)$ and in $H := L^2(\Omega)$. The elliptic regularity applies and provides constants $\sigma_{\text{reg}} > 1/2$, $\sigma := \min\{1, \sigma_{\text{reg}}\}$, and C_{reg} , which exclusively depend on Ω , such that, for any $j \in \mathbb{N}$, the eigenvector $\phi_j \in H^{2+\sigma_{\text{reg}}}(\Omega) \cap V$ is smooth and satisfies the regularity estimate

$$\|\phi_j\|_{H^{2+\sigma}(\Omega)} \leq C_{\text{reg}} \lambda_j$$

in the (possibly) broken Sobolev space $H^{2+\sigma}(\Omega)$ with the Sobolev-Slobodeckij norm $\|\bullet\|_{H^{2+\sigma}(\Omega)}$ [Gri85].

2.2. Discrete eigenvalue problem. Consider the family \mathbb{T} of regular triangulations (in the sense of Ciarlet) of the polygonal bounded Lipschitz domain $\Omega \subset \mathbb{R}^2$ obtained by newest vertex bisection (NVB) based on an initial triangulation $\mathcal{T}_{\text{init}}$ [BDD04, Ste08]. The shape-regularity of the initial triangulation $\mathcal{T}_{\text{init}}$ (that matches the domain exactly) transfers to any triangulation $\mathcal{T} \in \mathbb{T}$ uniformly. Given any $0 < \delta < 1$ (resp. $N \in \mathbb{N}_0$) we abbreviate $\mathbb{T}(\delta)$ (resp. $\mathbb{T}[N]$) as the subset of all $\mathcal{T} \in \mathbb{T}$ with maximal mesh-size $h_{\text{max}} \leq \delta$ (resp. with at most $N + |\mathcal{T}_0|$ triangles; here and throughout $|\mathcal{T}|$ is the cardinality of \mathcal{T} , that is the number of triangles in \mathcal{T}).

Each triangulation $\mathcal{T} \in \mathbb{T}$ defines a conforming finite element space $V(\mathcal{T}) \subset V$ of (finite) dimension $N \in \mathbb{N}$ and the associated discrete eigenvalue (2) problem seeks some discrete eigenpair $(\lambda_h, u_h) \in \mathbb{R}_+ \times V(\mathcal{T})$ for the number j . There are precisely N pairwise a -orthogonal and b -orthonormal discrete eigenvectors $\phi_h^{(1)}, \phi_h^{(2)}, \dots, \phi_h^{(N)} \in V(\mathcal{T})$ and those form a basis of $V(\mathcal{T})$. Any $j, k = 1, \dots, N$ satisfy

$$a(\phi_h^{(j)}, \psi_h) = \lambda_h^{(j)} b(\phi_h^{(j)}, \psi_h) \quad \text{for all } \psi_h \in V(\mathcal{T}), \quad a(\phi_h^{(j)}, \phi_h^{(k)}) = \lambda_h^{(j)} \delta_{jk}, \quad \text{and} \quad b(\phi_h^{(j)}, \phi_h^{(k)}) = \delta_{jk}.$$

Throughout this paper we assume an ascending enumeration $0 < \lambda_h^{(1)} \leq \lambda_h^{(2)} \leq \dots \leq \lambda_h^{(N)}$ of the associated eigenvalues counting multiplicities. A corollary of the Raleigh-Ritz min-max principle [BO91, Sec. 8] is the guaranteed upper bound property

$$(6) \quad \lambda_k \leq \lambda_h^{(k)} \quad \text{for all } k = 1, \dots, N.$$

2.3. A priori convergence. The first convergence results for elliptic eigenvalue problems in question date back to George Fix in 1973 and the old book [SF73] presents an a priori error analysis for the Laplacian; but the fairly general arguments apply to the present situation as well; other standard references include [BO91, Bof10]. In the above notation, let $\lambda := \lambda_j$ be a simple eigenvalue of number $j \in \mathbb{N}$, there exists positive constants δ_1 and Λ_{qo} such that the following holds for any triangulation $\mathcal{T} \in \mathbb{T}(\delta_1)$ with maximal mesh-size at most δ_1 . The dimension N of $V(\mathcal{T})$ is at least j and we simply drop the index j and abbreviate the discrete eigenpair $(\lambda_h^{(j)}, \phi_h^{(j)})$ as (λ_h, u_h) and the exact eigenpair (λ_j, ϕ_j) as (λ, u) with a possible change of signs in $u_h = \pm \phi_h^{(j)}$ so that $b(u, u_h) \geq 0$ and

$$(7) \quad \text{LB} := \| \|u - u_h\| \|^2 + \lambda_h - \lambda + \|u - u_h\|^2 \leq \Lambda_{\text{qo}} \min_{v_h \in V(\mathcal{T})} \| \|u - v_h\| \|^2 = \mathcal{O}(h_{\text{max}}^{2\sigma}).$$

Notice that $\lambda_h - \lambda \geq 0$ (by (6)) implies that all terms of the lower bound LB in (7) are non-negative.

Let us summarise the smallness assumptions on the mesh-sizes required so far. First some $\delta_1 > 0$ guarantees that the dimension $N := \dim V(\mathcal{T})$ of $V(\mathcal{T})$ is at least $j \in \mathbb{N}$ so that a discrete eigenpair (λ_h, u_h) of number $j \leq N$ exists whenever $\mathcal{T} \in \mathbb{T}(\delta_1)$. Second, we shall use that LB in (7) is small and we quantify this (with some possibly smaller δ_1) by

$$(8) \quad \text{LB} < 1/2 \quad \text{for all } \mathcal{T} \in \mathbb{T}(\delta_1).$$

This implies in particular that $b(u, u_h) = 1 - 1/2 \|u - u_h\|^2 \geq 3/4$ (from the binomial theorem and $\|u\| = 1 = \|u_h\|$) is at least $3/4$ and the sign of $u_h = \pm \phi_h^{(j)}$ is uniquely determined by that of u .

We need some further smallness of LB for uniform separation of eigenvalues. The resolution of the spectral gap $\lambda_{j-1} < \lambda \equiv \lambda_j < \lambda_{j+1}$ of the simple eigenvalue λ with the number $j \in \mathbb{N}$ (and the convention $\lambda_0 := \lambda_h^{(0)} := 0$) by the discrete counterparts $\lambda_h^{(j-1)} \leq \lambda_h^{(j)} \equiv \lambda_h \leq \lambda_h^{(j+1)}$ requires

$$(9) \quad \lambda_{j-1} \leq \lambda_h^{(j-1)} < \lambda_j \equiv \lambda \leq \lambda_h^{(j)} \equiv \lambda_h < \lambda_{j+1} \leq \lambda_h^{(j+1)},$$

where the positive gaps $\lambda - \lambda_h^{(j-1)}$ and $\lambda_{j+1} - \lambda_h$ are bounded below by a positive constant. This follows from (7) for sufficiently small mesh-sizes h_{max} and leads to some positive $\delta_2 \leq \delta_1$ such that (9) holds for

all $\mathcal{T} \in \mathbb{T}(\delta_2)$. Consequently, the lower bounds of the weighted gaps provides the boundedness

$$(10) \quad \max\left\{\frac{\lambda_j}{\lambda_j - \lambda_h^{(j-1)}}, \frac{\lambda_h^{(j)}}{\lambda_h^{(j+1)} - \lambda_h^{(j)}}\right\} \leq \Lambda_{\text{sep}}$$

with some positive separation constant $\Lambda_{\text{sep}} < \infty$ that is independent of $\mathcal{T} \in \mathbb{T}(\delta_2)$. Separation conditions frequently appear in an eigenvalue convergence analysis and we note that (10) implies in particular that

$$\sup_{\mathcal{T} \in \mathbb{T}(\delta_2)} \max_{k \neq j} \frac{\lambda_h^{(j)}}{|\lambda_h^{(k)} - \lambda_h^{(j)}|} \leq \Lambda_{\text{sep}} \quad \text{and} \quad \sup_{\mathcal{T} \in \mathbb{T}(\delta_2)} \max_{k \neq j} \frac{\lambda_j}{|\lambda_h^{(k)} - \lambda_j|} \leq \Lambda_{\text{sep}}$$

(with the abbreviation $\max_{k \neq j}$ for the maximum over all $k \in \{1, \dots, N\} \setminus \{j\}$ with $N := \dim V(\mathcal{T})$). In fact, the monotonicity and $\lambda \leq \lambda_h$ imply the missing part $\lambda_h/(\lambda_h - \lambda_h^{(j-1)}) \leq \lambda/(\lambda - \lambda_h^{(j-1)}) \leq \Lambda_{\text{sep}}$ of the first estimate; the proof of the second is analogous.

There are extensions of (7) to multiple eigenvalues with reduced convergence [SF73], but then the notation is significantly more technical and the analog analysis of the cluster algorithm [Gal15] remains for future research.

2.4. Two-level notation. Throughout this paper, let $j \in \mathbb{N}$ denote the fixed number of a simple eigenvalue $\lambda \equiv \lambda_j$ and assume that the positive constants $\delta_2 \leq \delta_1$, Λ_{qo} , and Λ_{sep} satisfy (7)-(10). Consider an admissible refinement $\widehat{\mathcal{T}}$ of $\mathcal{T} \in \mathbb{T}(\delta_2)$ and let $(\lambda_h, u_h) \in \mathbb{R}^+ \times V(\mathcal{T})$ resp. $(\widehat{\lambda}_h, \widehat{u}_h) \in \mathbb{R}^+ \times V(\widehat{\mathcal{T}})$ denote the respective discrete eigenpair number j of (2). Recall that (7)–(8) uniquely determines (the orientation of) those discrete eigenvectors. Another corollary of the Rayleigh-Ritz min-max principle [BO91, Sec. 8] (on the algebraic level) and $V(\mathcal{T}) \subset V(\widehat{\mathcal{T}})$ reads $\widehat{\lambda}_h \leq \lambda_h$ and so $\lambda \leq \widehat{\lambda}_h \leq \lambda_h$ in addition to (9).

The key to any a priori or a posteriori error analysis is the uniform smallness of the H norm compared to the V norm of the error term $\widehat{e} := \widehat{u}_h - u_h$.

Lemma 2.1 (key). *There exists a constant Λ_{stab} , that exclusively depends on $\Lambda_{\text{sep}}, \Omega, \sigma, \delta_2$, and \mathbb{T} , but not on $\mathcal{T} \in \mathbb{T}(\delta_2)$ with maximal mesh-size $h_{\text{max}} \leq \delta_2$, such that*

$$\|\widehat{u}_h - u_h\| \leq \Lambda_{\text{stab}} h_{\text{max}}^\sigma \|\widehat{u}_h - u_h\|.$$

Proof. The lemma is indicated in [CFPP14] for the Laplace eigenvalue problem, but the proof is merely outlined. The more detailed proof below has eight steps. *The first step* verifies a 2-level separation condition

$$(11) \quad \sup_{\mathcal{T} \in \mathbb{T}(\delta_2)} \max_{k \neq j} \frac{\widehat{\lambda}_h}{|\lambda_h^{(k)} - \widehat{\lambda}_h|} \leq \Lambda_{\text{sep}}.$$

The proof of (11) follows by monotonicity and the relations $\lambda \leq \widehat{\lambda}_h \leq \lambda_h$ in the 2-level notation:

$$\frac{\widehat{\lambda}_h}{\lambda_h^{(j+1)} - \widehat{\lambda}_h} \leq \frac{\lambda_h}{\lambda_h^{(j+1)} - \lambda_h} \leq \Lambda_{\text{sep}} \quad \text{and} \quad \frac{\widehat{\lambda}_h}{\widehat{\lambda}_h - \lambda_h^{(j-1)}} \leq \frac{\lambda}{\lambda - \lambda_h^{(j-1)}} \leq \Lambda_{\text{sep}}.$$

The second step concerns the Galerkin projection $G \in L(V)$ onto $V(\mathcal{T})$ with

$$(12) \quad Gv \in V(\mathcal{T}) \quad \text{and} \quad a(v - Gv, v_h) = 0 \quad \text{for all } (v, v_h) \in V \times V(\mathcal{T}).$$

The approximation properties are well established and a standard duality argument reveals

$$(13) \quad \|v - Gv\| \leq \Lambda_{\text{dual}} h_{\text{max}}^\sigma \|v - Gv\| \quad \text{for all } v \in V$$

with a universal constant Λ_{dual} that exclusively depends on σ, Ω , and \mathbb{T} , but is independent of $\mathcal{T} \in \mathbb{T}$ and v . Further details can be found in [Cia02, SF73, EG17, BS08].

The third step introduces the H projection $G\widehat{u}_h - \gamma u_h$ of $G\widehat{u}_h$ onto the span of u_h with the Fourier coefficient $\gamma := b(G\widehat{u}_h, u_h)$. Since the discrete vector $G\widehat{u}_h - \gamma u_h \in V(\mathcal{T})$ belongs to the coarse finite element space $V(\mathcal{T})$ of dimension N , it has a Fourier expansion with the eigenvectors $\phi_h^{(k)}$ and coefficients $\alpha_k := b(G\widehat{u}_h - \gamma u_h, \phi_h^{(k)}) \in \mathbb{R}$ for $k = 1, \dots, N$. The orthogonality of the discrete eigenvectors implies $\alpha_j = 0$ and $\alpha_k = b(G\widehat{u}_h, \phi_h^{(k)})$ for $k \neq j$. Consequently, the finite Fourier series

$$G\widehat{u}_h - \gamma u_h = \sum_{k \neq j} \alpha_k \phi_h^{(k)}$$

leads to the H norm identity

$$\|G\widehat{u}_h - \gamma u_h\|^2 = \sum_{k \neq j} \alpha_k^2.$$

The *fourth step* performs the critical spectral analysis with the discrete eigenvalue problem (2) for an eigenpair $(\lambda_h^{(k)}, \phi_h^{(k)})$ of number $k \neq j$ with $\alpha_k = b(G\widehat{u}_h, \phi_h^{(k)})$. Therefore, (2) and (12) provide

$$\lambda_h^{(k)} \alpha_k = a(G\widehat{u}_h, \phi_h^{(k)}) = a(\widehat{u}_h, \phi_h^{(k)}).$$

Since $(\widehat{\lambda}_h, \widehat{u}_h)$ is an eigenpair on the fine level and $V(\mathcal{T}) \subset V(\widehat{\mathcal{T}})$, $a(\widehat{u}_h, \phi_h^{(k)}) = \widehat{\lambda}_h b(\widehat{u}_h, \phi_h^{(k)})$. Thus

$$(\lambda_h^{(k)} - \widehat{\lambda}_h) \alpha_k = \widehat{\lambda}_h b(\widehat{u}_h - G\widehat{u}_h, \phi_h^{(k)}) = \widehat{\lambda}_h \beta_k$$

with the abbreviation $\beta_k := b(\widehat{u}_h - G\widehat{u}_h, \phi_h^{(k)}) \in \mathbb{R}$, $k \neq j$. This reads $\alpha_k = \widehat{\lambda}_h \beta_k / (\lambda_h^{(k)} - \widehat{\lambda}_h)$ such that

$$|\alpha_k| \leq \Lambda_{\text{sep}} |\beta_k| \quad \text{for all } k \neq j$$

follows from (11) and establishes the intermediate bound

$$\|G\widehat{u}_h - \gamma u_h\|^2 = \sum_{k \neq j} \alpha_k^2 \leq \Lambda_{\text{sep}}^2 \sum_{k \neq j} \beta_k^2.$$

Step five starts with a Bessel inequality for the Fourier coefficients $\beta_k = b(\widehat{u}_h - G\widehat{u}_h, \phi_h^{(k)})$, namely

$$\sum_{k \neq j} \beta_k^2 \leq \|\widehat{u}_h - G\widehat{u}_h\|^2.$$

The synopsis with the previous step and thereafter (13) verify

$$\|G\widehat{u}_h - \gamma u_h\| \leq \Lambda_{\text{sep}} \|\widehat{u}_h - G\widehat{u}_h\| \leq \Lambda_{\text{sep}} \Lambda_{\text{dual}} h_{\text{max}}^\sigma \|\widehat{u}_h - G\widehat{u}_h\|.$$

Since the Galerkin projection (12) is a best-approximation, $\|\widehat{u}_h - G\widehat{u}_h\| \leq \|\widehat{u}_h - u_h\| = \|\widehat{e}\|$ results in

$$(14) \quad \|G\widehat{u}_h - \gamma u_h\| \leq \Lambda_{\text{sep}} \Lambda_{\text{dual}} h_{\text{max}}^\sigma \|\widehat{e}\|.$$

Step six clarifies $\beta := b(\widehat{u}_h, u_h) \geq 0$. The binomial theorem and $\|\widehat{u}_h\| = 1 = \|u_h\|$ reveal

$$2(1 - \beta) = \|\widehat{e}\|^2 \leq (\|u - \widehat{u}_h\| + \|u - u_h\|)^2 \leq 2$$

with a triangle inequality and $\|u - \widehat{u}_h\|, \|u - u_h\| \leq 2^{-1/2}$ from (8) in the last step. Hence $0 \leq \beta$.

Step seven proves $\|\widehat{e}\| \leq \sqrt{2} \|\widehat{u}_h - \gamma u_h\|$ by elementary algebra and $\|\widehat{u}_h\| = 1 = \|u_h\|$. Indeed, direct calculations with $0 \leq \beta := b(\widehat{u}_h, u_h) \leq 1$ in the last estimate result in

$$\|\widehat{e}\|^2 / 2 = 1 - \beta = \|\widehat{u}_h - \beta u_h\|^2 / (1 + \beta) \leq \|\widehat{u}_h - \beta u_h\|^2.$$

This and $\|\widehat{u}_h - \beta u_h\| = \min_{t \in \mathbb{R}} \|\widehat{u}_h - t u_h\|$ from $\|\widehat{u}_h - t u_h\|^2 = 1 - 2t\beta + t^2$ read

$$(15) \quad 2^{-1/2} \|\widehat{e}\| \leq \min_{t \in \mathbb{R}} \|\widehat{u}_h - t u_h\| \leq \|\widehat{u}_h - \gamma u_h\|.$$

Step eight concludes the proof. Recall (15) and employ a triangle inequality to infer

$$2^{-1/2} \|\widehat{e}\| \leq \|\widehat{u}_h - \gamma u_h\| \leq \|\widehat{u}_h - G\widehat{u}_h\| + \|G\widehat{u}_h - \gamma u_h\|.$$

The terms $\|\widehat{u}_h - G\widehat{u}_h\|$ and $\|G\widehat{u}_h - \gamma u_h\|$ are controlled by (13)–(14). The combination with $\|\widehat{u}_h - G\widehat{u}_h\| \leq \|\widehat{e}\|$ (from best-approximation of G) leads to

$$2^{-1/2} \|\widehat{e}\| \leq (1 + \Lambda_{\text{sep}}) \Lambda_{\text{dual}} h_{\text{max}}^\sigma \|\widehat{e}\|.$$

This is the assertion for $\Lambda_{\text{stab}} := \sqrt{2}(1 + \Lambda_{\text{sep}}) \Lambda_{\text{dual}}$. \square

2.5. Discrete reliability analysis. Given the 2-level notation of Subsection 2.4 with the fine and coarse discrete eigenpair $(\widehat{\lambda}_h, \widehat{u}_h) \in \mathbb{R}_+ \times V(\widehat{\mathcal{T}})$ and $(\lambda_h, u_h) \in \mathbb{R}_+ \times V(\mathcal{T})$, respectively, and the error $\widehat{e} := \widehat{u}_h - u_h \in V(\widehat{\mathcal{T}})$, consider the linear bounded functional $\text{Res} \in V^*$ on the coarse level by

$$(16) \quad \text{Res}(\varphi) := \lambda_h b(u_h, \varphi) - a(u_h, \varphi) \quad \text{for all } \varphi \in V.$$

Observe that the solution property (2) for the coarse eigenpair $(\lambda_h, u_h) \in \mathbb{R}_+ \times V(\mathcal{T})$ implies $\text{Res}(v_h) = 0$ for all $v_h \in V(\mathcal{T})$, written $V(\mathcal{T}) \subset \ker \text{Res}$. The latter property enables a classical explicit residual-based a posteriori error analysis and allows below the derivation of computable reliable upper bounds of

$$\|\text{Res}\|_{V(\widehat{\mathcal{T}})^*} := \sup_{\widehat{v}_h \in V(\widehat{\mathcal{T}}) \setminus \{0\}} \text{Res}(\widehat{v}_h) / \|\widehat{v}_h\| \leq \|\text{Res}\|_* := \|\text{Res}\|_{V^*} := \sup_{v \in V \setminus \{0\}} \text{Res}(v) / \|v\|.$$

Given any parameter $0 < \kappa < 1$, set $\delta_3 := \min\{\delta_2, (\kappa / (\lambda_{j+1} \Lambda_{\text{stab}}^2))^{1/(2\sigma)}\}$ and suppose $\mathcal{T} \in \mathbb{T}(\delta_3)$.

Lemma 2.2 (2-level a posteriori error estimation). *Under the 2-level notation with $\mathcal{T} \in \mathbb{T}(\delta_3)$, it holds*

$$(a) \quad (1 - \kappa) \|\widehat{e}\|^2 \leq \text{Res}(\widehat{e}) \leq \lambda_h - \widehat{\lambda}_h \leq \|\widehat{e}\|^2 \quad \text{and} \quad (b) \quad (1 - \kappa) \|\widehat{e}\| \leq \|\text{Res}\|_{V(\widehat{\mathcal{T}})^*} \leq 2 \|\widehat{e}\|.$$

Proof of Lemma 2.2.a. The role of the residual becomes clear in a little calculation with the fine eigenpair $(\widehat{\lambda}_h, \widehat{u}_h)$ and the error $\widehat{e} \in V(\widehat{\mathcal{T}})$,

$$(17) \quad \|\widehat{e}\|^2 = a(\widehat{u}_h - u_h, \widehat{e}) = \widehat{\lambda}_h b(\widehat{u}_h, \widehat{e}) - a(u_h, \widehat{e}) = \text{Res}(\widehat{e}) + b(\widehat{\lambda}_h \widehat{u}_h - \lambda_h u_h, \widehat{e}).$$

It remains to control the nonlinear contribution $b(\widehat{\lambda}_h \widehat{u}_h - \lambda_h u_h, \widehat{e})$ with elementary algebra and the key lemma. The binomial theorem and $\|\widehat{u}_h\| = 1 = \|u_h\|$ imply $b(\widehat{u}_h + u_h, \widehat{u}_h - u_h) = 0$. This and $2(\widehat{\lambda}_h \widehat{u}_h - \lambda_h u_h) = (\widehat{\lambda}_h + \lambda_h)\widehat{e} + (\widehat{\lambda}_h - \lambda_h)(\widehat{u}_h + u_h)$ verify

$$(18) \quad 2b(\widehat{\lambda}_h \widehat{u}_h - \lambda_h u_h, \widehat{e}) = b((\widehat{\lambda}_h + \lambda_h)\widehat{e} + (\widehat{\lambda}_h - \lambda_h)(\widehat{u}_h + u_h), \widehat{e}) = (\widehat{\lambda}_h + \lambda_h)\|\widehat{e}\|^2.$$

Therefore, (17) reads

$$(19) \quad \|\widehat{e}\|^2 = \text{Res}(\widehat{e}) + (\widehat{\lambda}_h + \lambda_h)/2 \|\widehat{e}\|^2.$$

The additional assumption $\mathcal{T} \in \mathbb{T}(\delta_3)$ provides $h_{\max}^{2\sigma} \lambda_{j+1} \Lambda_{\text{stab}}^2 \leq \kappa$, so that $(\widehat{\lambda}_h + \lambda_h)/2 \leq \lambda_{j+1}$ by (9) leads in the key Lemma 2.1 to

$$(20) \quad (\widehat{\lambda}_h + \lambda_h)/2 \|\widehat{e}\|^2 \leq \kappa \|\widehat{e}\|^2.$$

The combination of (19)–(20) results in $(1 - \kappa)\|\widehat{e}\|^2 \leq \text{Res}(\widehat{e}) \leq \|\widehat{e}\|^2$ as part of the assertions. The remaining statements follow with the well known Pythagorean theorem for eigenpairs

$$(21) \quad \|\widehat{e}\|^2 = \lambda_h - \widehat{\lambda}_h + \widehat{\lambda}_h \|\widehat{e}\|^2.$$

This 2-level version is stated and proven in [CFPP14, Lem. 10.6] for the Laplace operator, but the direct algebraic proof for the situation at hand is the same and hence not repeated. Recall the key Lemma 2.1 for $\lambda_{j+1}\|\widehat{e}\|^2 \leq \kappa\|\widehat{e}\|^2$ and $\widehat{\lambda}_h \leq \lambda_{j+1}$ (from (9)) to deduce with (21) that

$$0 \leq \|\widehat{e}\|^2 - (\lambda_h - \widehat{\lambda}_h) = \widehat{\lambda}_h \|\widehat{e}\|^2 \leq \kappa \|\widehat{e}\|^2.$$

This is another part of the assertions, namely $(1 - \kappa)\|\widehat{e}\|^2 \leq \lambda_h - \widehat{\lambda}_h \leq \|\widehat{e}\|^2$. The combination of (19) and (21) results in $\text{Res}(\widehat{e}) = (\lambda_h - \widehat{\lambda}_h)(1 - \|\widehat{e}\|^2/2) \leq \lambda_h - \widehat{\lambda}_h$ and concludes the proof of (a). \square

Proof of Lemma 2.2.b. Step one analyses the Riesz representation \widehat{v} of Res. Let $\widehat{v} \in V(\widehat{\mathcal{T}})$ denote the Riesz representation of $\text{Res} = a(\widehat{v}, \bullet)$ in the Hilbert space $(V(\widehat{\mathcal{T}}), a)$ and deduce $G\widehat{v} = 0$ for the Galerkin projection (12) from

$$\|G\widehat{v}\|^2 = a(\widehat{v}, G\widehat{v}) = \text{Res}(G\widehat{v}) = 0 \quad \text{by } G\widehat{v} \in V(\mathcal{T}) \subset \ker \text{Res}.$$

The duality estimate (13) and $h_{\max}^\sigma \leq \Lambda_{\text{stab}}^{-1} \sqrt{\kappa/\lambda_{j+1}}$ from $\mathcal{T} \in \mathbb{T}(\delta_3)$ in the last step provide

$$\|\widehat{v}\| = \|\widehat{v} - G\widehat{v}\| \leq \Lambda_{\text{dual}} h_{\max}^\sigma \|\widehat{v}\| \leq \Lambda_{\text{dual}} \Lambda_{\text{stab}}^{-1} \sqrt{\kappa/\lambda_{j+1}} \|\widehat{v}\|.$$

Recall $\Lambda_{\text{stab}} = \sqrt{2}(1 + \Lambda_{\text{sep}})\Lambda_{\text{dual}}$ from the key Lemma 2.1 to recast this as

$$(22) \quad \|\widehat{v}\| \leq (1 + \Lambda_{\text{sep}})^{-1} \sqrt{\kappa/(2\lambda_{j+1})} \|\widehat{v}\|.$$

Step two controls the nonlinear term $\|\widehat{\lambda}_h \widehat{u}_h - \lambda_h u_h\|$. The arguments, which led above to (18), also verify

$$4\|\widehat{\lambda}_h \widehat{u}_h - \lambda_h u_h\|^2 - (\widehat{\lambda}_h + \lambda_h)^2 \|\widehat{e}\|^2 = (\lambda_h - \widehat{\lambda}_h)^2 \|\widehat{u}_h + u_h\|^2 \leq 4(\lambda_h - \widehat{\lambda}_h)^2.$$

Recall (20) to rewrite this with part (a) as

$$\|\widehat{\lambda}_h \widehat{u}_h - \lambda_h u_h\|^2 \leq \left((\widehat{\lambda}_h + \lambda_h)\kappa/2 + \lambda_h - \widehat{\lambda}_h \right) \|\widehat{e}\|^2 \leq \lambda_{j+1}(1 + \kappa/2) \|\widehat{e}\|^2$$

with $\lambda_h \leq \lambda_{j+1}$ (from (9)) in the last step. In other words,

$$(23) \quad \|\widehat{\lambda}_h \widehat{u}_h - \lambda_h u_h\| \leq \sqrt{\lambda_{j+1}(1 + \kappa/2)} \|\widehat{e}\|.$$

Step three concludes the proof. The Riesz representation \widehat{v} with isometry $\|\text{Res}\|_{V(\widehat{\mathcal{T}})^*} = \|\widehat{v}\|$ satisfies

$$\|\widehat{v}\|^2 = \text{Res}(\widehat{v}) = b(\lambda_h u_h, \widehat{v}) - a(u_h, \widehat{v}) = b(\lambda_h u_h - \widehat{\lambda}_h \widehat{u}_h, \widehat{v}) + a(\widehat{e}, \widehat{v})$$

with the fine eigenpair $(\widehat{\lambda}_h, \widehat{u}_h)$ and the error $\widehat{e} \in V(\widehat{\mathcal{T}})$ in the last step. Cauchy inequalities and the estimates (22)–(23) reveal

$$\|\widehat{v}\|^2 \leq \left(1 + (1 + \Lambda_{\text{sep}})^{-1} \sqrt{(1 + \kappa/2)\kappa/2} \right) \|\widehat{e}\| \|\widehat{v}\|.$$

This proves a sharper version of the asserted estimate $\|\widehat{v}\| \leq 2\|\widehat{e}\|$. The remaining assertion follows from part (a) and the definition of the operator norm $\|\text{Res}\|_{V(\widehat{\mathcal{T}})^*}: (1 - \kappa)\|\widehat{e}\|^2 \leq \text{Res}(\widehat{e}) \leq \|\text{Res}\|_{V(\widehat{\mathcal{T}})^*} \|\widehat{e}\|$. \square

The emphasis of the a posteriori error analysis in this subsection is on the universal constants for a large class of triangulations, i.e., to allow δ_3 as large as possible. The other extreme when $h_{\max} \leq \delta_3$ tends to zero (e.g., from uniform refinement) remains undisplayed, but is worth a comment.

Remark (asymptotic exactness). If the maximal mesh-size h_{\max} of \mathcal{T} becomes smaller and tends to zero, the quantities $\text{Res}(\hat{e})$, $\lambda_h - \hat{\lambda}_h$, $\|\hat{e}\|^2$, and $\|\text{Res}\|_{V(\hat{\mathcal{T}})^*}$ are asymptotically exact in the sense that their pairwise quotients converge towards one. This follows essentially from the analysis in this subsection with the key Lemma 2.1 from $\kappa \rightarrow 0$ as $\delta_3 \rightarrow 0$ and has been observed before in Laplace eigenvalue problems [CG11].

3. ARGYRIS FEM FOR EIGENVALUE PROBLEMS

This section introduces the notation for the standard and hierarchical Argyris FEM.

3.1. Triangulations and Argyris finite element spaces. The Argyris finite element of degree $p = 5, 6, 7, \dots$ is well established and could be defined on a regular triangulation \mathcal{T} with set of vertices \mathcal{V} of the polygonal bounded Lipschitz domain $\Omega \subset \mathbb{R}^2$ by

$$(24) \quad A_p(\mathcal{T}) := \{v_h \in P_p(\mathcal{T}) \cap V : D^2 v_h \text{ is continuous at every } z \in \mathcal{V}\}.$$

This Argyris finite element space from [AFS68, BS05] is nowadays textbook topic [Bra07, BS08, BC17, Cia02] and we apply the hierarchical Argyris finite element method from [CH21]. Given a sequence of successive one-level refinements $\mathcal{T}_0, \mathcal{T}_1, \mathcal{T}_2, \dots$ of the initial triangulation \mathcal{T}_0 by the newest-vertex bisection (NVB) (where each triangle is divided in at most four sub-triangles via bisection of refinement edges), the spaces

$$(25) \quad V(\mathcal{T}_\ell) := A_p(\mathcal{T}_0) + A_p(\mathcal{T}_1) + \dots + A_p(\mathcal{T}_\ell) \quad \text{for any } \ell \in \mathbb{N}_0$$

are obviously conforming and nested. It can be shown that $V(\mathcal{T}_\ell)$ exclusively depends on \mathcal{T}_ℓ (and does not depend on the the sequence $\mathcal{T}_0, \mathcal{T}_1, \mathcal{T}_2, \dots, \mathcal{T}_\ell$). This and a characterisation of the nodal basis in the extended Argyris finite element space $V(\mathcal{T}_\ell)$ are provided in [CH21, Grä22, CG24].

Let \mathbb{T} denote the set of all triangulations \mathcal{T}_ℓ generated in the NVB and given $\mathcal{T} \in \mathbb{T}$ some refinement $\hat{\mathcal{T}} \in \mathbb{T}(\mathcal{T})$ thereof, adopt the 2-level notation of Subsection 2.4 with discrete eigenpairs $(\lambda_h, u_h) \in \mathbb{R}^+ \times V(\mathcal{T})$ resp. $(\hat{\lambda}_h, \hat{u}_h) \in \mathbb{R}^+ \times V(\hat{\mathcal{T}})$ of fixed number j of (2); set $\hat{e} := \hat{u}_h - u_h \in V(\hat{\mathcal{T}})$ and

$$\delta(\mathcal{T}, \hat{\mathcal{T}}) := \|\hat{e}\|.$$

The subsequent subsections provide some properties (A1)–(A4) sufficient for optimal convergence rates of AFEM [CFPP14, CR17, CH21].

3.2. Proof of stability (A1). The error estimator (3) is based on the coarse level of the 2-level notation of Subsection 2.4. Its counterpart on the fine level with the discrete eigenpair $(\hat{\lambda}_h, \hat{u}_h) \in \mathbb{R}^+ \times V(\hat{\mathcal{T}})$ is $\hat{\eta}^2(\mathcal{T}) := \sum_{T \in \hat{\mathcal{T}}} \hat{\eta}^2(T)$ based on the triangulation $\hat{\mathcal{T}} \in \mathbb{T}(\delta_2)$ and the contribution

$$(26) \quad \hat{\eta}^2(T) = |T|^2 \|\widehat{\lambda}_h \widehat{u}_h - \Delta^2 \widehat{u}_h\|_{L^2(T)}^2 + |T|^{1/2} \|[\partial_{\nu\nu}^2 \widehat{u}_h]_E\|_{L^2(\partial T \cap \Omega)}^2 + |T|^{3/2} \|[\partial_\nu \Delta \widehat{u}_h]_E\|_{L^2(\partial T \cap \Omega)}^2$$

for each $T \in \hat{\mathcal{T}}$. Recall that $\hat{\mathcal{T}}$ is a refinement of \mathcal{T} , whence $\mathcal{T} \cap \hat{\mathcal{T}}$ is the (possibly empty) set of coarse and fine triangles. The sum convention defines $\eta(\mathcal{T} \cap \hat{\mathcal{T}})$ (resp. $\hat{\eta}(\mathcal{T} \cap \hat{\mathcal{T}})$) as the square root of $\eta^2(\mathcal{T} \cap \hat{\mathcal{T}}) := \sum_{T \in \mathcal{T} \cap \hat{\mathcal{T}}} \eta^2(T)$ (resp. $\hat{\eta}^2(\mathcal{T} \cap \hat{\mathcal{T}}) := \sum_{T \in \mathcal{T} \cap \hat{\mathcal{T}}} \hat{\eta}^2(T)$). Error estimator stability has been observed [CFPP14, CKNS08] for many estimators and asserts in the 2-level notation at hand that

$$(A1) \quad |\hat{\eta}(\mathcal{T} \cap \hat{\mathcal{T}}) - \eta(\mathcal{T} \cap \hat{\mathcal{T}})| \leq \Lambda_1 \delta(\mathcal{T}, \hat{\mathcal{T}}).$$

The slightly technical proof of stability (A1) utilizes reverse triangle inequalities and is well-established by now. For instance, the corresponding analysis in [CH21] is completely omitted. We therefore give an outline of the arguments and emphasise the nonlinearity. Indeed, the term $\eta(T)$ for $T \in \mathcal{T}$ is the Euclidean norm of a vector with the entries $|T| \|\lambda_h u_h - \Delta^2 u_h\|_{L^2(T)}$ as well as $|T|^{1/4} \|[\partial_{\nu\nu}^2 u_h]_E\|_{L^2(E)}$ and $|T|^{3/4} \|[\partial_\nu \Delta u_h]_E\|_{L^2(E)}$ for all $E \in \mathcal{E}(T) \cap \mathcal{E}(\Omega)$. The same interpretation of $\hat{\eta}(T)$ for $T \in \hat{\mathcal{T}}$ considers $\eta(\mathcal{T} \cap \hat{\mathcal{T}})$ and $\hat{\eta}(\mathcal{T} \cap \hat{\mathcal{T}})$ as Euclidean norms of vectors of the same length $m \in \mathbb{N}_0$. Hence the squares of

the reverse triangle inequality in \mathbb{R}^m result in

$$\begin{aligned} \left| \widehat{\eta}(\mathcal{T} \cap \widehat{\mathcal{T}}) - \eta(\mathcal{T} \cap \widehat{\mathcal{T}}) \right|^2 &\leq \sum_{T \in \mathcal{T} \cap \widehat{\mathcal{T}}} |T|^2 \left| \|\lambda_h u_h - \Delta^2 u_h\|_{L^2(T)} - \|\widehat{\lambda}_h \widehat{u}_h - \Delta^2 \widehat{u}_h\|_{L^2(T)} \right|^2 \\ &+ \sum_{T \in \mathcal{T} \cap \widehat{\mathcal{T}}} |T|^{1/2} \sum_{E \in \mathcal{E}(T) \setminus \mathcal{E}(\Omega)} \left| \|\partial_{\nu\nu}^2 \widehat{u}_h\|_E - \|\partial_{\nu\nu}^2 u_h\|_E \right|^2 \\ &+ \sum_{T \in \mathcal{T} \cap \widehat{\mathcal{T}}} |T|^{3/2} \sum_{E \in \mathcal{E}(T) \setminus \mathcal{E}(\Omega)} \left| \|\partial_\nu \Delta \widehat{u}_h\|_E - \|\partial_\nu \Delta u_h\|_E \right|^2. \end{aligned}$$

The reverse triangle inequality in $L^2(T)$ resp. $L^2(E)$ allows for the upper bound

$$(27) \quad \begin{aligned} \left| \widehat{\eta}(\mathcal{T} \cap \widehat{\mathcal{T}}) - \eta(\mathcal{T} \cap \widehat{\mathcal{T}}) \right|^2 &\leq \sum_{T \in \mathcal{T} \cap \widehat{\mathcal{T}}} |T|^2 \|\widehat{\lambda}_h \widehat{u}_h - \lambda_h u_h - \Delta^2 \widehat{e}\|_{L^2(T)}^2 \\ &+ \sum_{T \in \mathcal{T} \cap \widehat{\mathcal{T}}} |T|^{1/2} \sum_{E \in \mathcal{E}(T) \setminus \mathcal{E}(\Omega)} \|\partial_{\nu\nu}^2 \widehat{e}\|_E^2 + \sum_{T \in \mathcal{T} \cap \widehat{\mathcal{T}}} |T|^{3/2} \sum_{E \in \mathcal{E}(T) \setminus \mathcal{E}(\Omega)} \|\partial_\nu \Delta \widehat{e}\|_E^2. \end{aligned}$$

The three sums in the upper bound are treated separately and the non-linear volume terms

$$|T|^2 \|\widehat{\lambda}_h \widehat{u}_h - \lambda_h u_h - \Delta^2 \widehat{e}\|_{L^2(T)}^2 \leq 2|T|^2 \|\widehat{\lambda}_h \widehat{u}_h - \lambda_h u_h\|_{L^2(T)}^2 + 2|T|^2 \|\Delta^2 \widehat{e}\|_{L^2(T)}^2$$

in the first sum over $T \in \mathcal{T} \cap \widehat{\mathcal{T}}$ deserve special attention. An inverse estimate in the last term leads to some positive constant C_{inv} (which exclusively depends on the shape-regularity in \mathbb{T} and the polynomial degree in the finite element space $V(\mathcal{T})$) in

$$|T| \|\Delta^2 \widehat{e}\|_{L^2(T)} \leq C_{\text{inv}} |\widehat{e}|_{H^2(T)}.$$

The nonlinear term is estimated in (23) and reveals

$$2 \sum_{T \in \mathcal{T} \cap \widehat{\mathcal{T}}} |T|^2 \|\widehat{\lambda}_h \widehat{u}_h - \lambda_h u_h\|_{L^2(T)}^2 \leq h_{\max}^4 / 2 \|\widehat{\lambda}_h \widehat{u}_h - \lambda_h u_h\|^2 \leq h_{\max}^4 \lambda_{j+1} (2 + \kappa) / 8 \|\widehat{e}\|^2.$$

The combination of the previous two displayed estimates leads to

$$\sum_{T \in \mathcal{T} \cap \widehat{\mathcal{T}}} |T|^2 \|\widehat{\lambda}_h \widehat{u}_h - \lambda_h u_h - \Delta^2 \widehat{e}\|_{L^2(T)}^2 \leq (h_{\max}^4 \lambda_{j+1} (2 + \kappa) / 8 + 2C_{\text{inv}}^2) \|\widehat{e}\|^2.$$

The routine estimation by triangle, trace, and inverse inequalities as in [CH21, Grä22] for the source problem eventually bounds the jump terms in (27) by $\Lambda_1^2 \|\widehat{e}\|^2$. This and the previous displayed estimate in (27) conclude the proof of (A1) with $\Lambda_1 := \sqrt{\Lambda_1'^2 + \delta_2^4 \lambda_{j+1} (2 + \kappa) / 8 + 2C_{\text{inv}}^2}$. \square

3.3. Proof of reduction (A2). Adopt the setting of the previous subsection and consider the set $\mathcal{T} \setminus \widehat{\mathcal{T}}$ of coarse but not fine triangles together with the fine but not coarse triangles in $\widehat{\mathcal{T}} \setminus \mathcal{T}$. The sum convention defines the two related estimator terms $\eta(\mathcal{T} \setminus \widehat{\mathcal{T}})$ resp. $\widehat{\eta}(\widehat{\mathcal{T}} \setminus \mathcal{T})$ on the coarse resp. fine level. The aim of this subsection is the proof of the error estimator reduction

$$(A2) \quad \widehat{\eta}(\widehat{\mathcal{T}} \setminus \mathcal{T}) \leq 2^{-1/4} \eta(\mathcal{T} \setminus \widehat{\mathcal{T}}) + \Lambda_2 \delta(\mathcal{T}, \widehat{\mathcal{T}}).$$

The main arguments are those from the previous section and in fact $\Lambda_2 = \Lambda_1$. But the details are more involved and perhaps simplified with auxiliary estimator terms $\widetilde{\eta}^2(T)$ defined for each fine triangle $T \in \widehat{\mathcal{T}}$ with respect to the coarse eigenpair $(\lambda_h, u_h) \in \mathbb{R}^+ \times V(\mathcal{T})$, i.e.,

$$(28) \quad \begin{aligned} \widetilde{\eta}^2(T) &= |T|^2 \|\lambda_h u_h - \Delta^2 u_h\|_{L^2(T)}^2 \\ &+ |T|^{1/2} \sum_{E \in \widehat{\mathcal{E}}(T) \setminus \widehat{\mathcal{E}}(\Omega)} \|\partial_{\nu\nu}^2 u_h\|_E^2 + |T|^{3/2} \sum_{E \in \widehat{\mathcal{E}}(T) \setminus \widehat{\mathcal{E}}(\Omega)} \|\partial_\nu \Delta u_h\|_E^2. \end{aligned}$$

Notice the same index sets over the triangle and edges with respect to the fine geometry of $\widehat{\mathcal{T}}$ in (26) and (28). Reverse triangle inequalities lead (in \mathbb{R}^m and in $L^2(T)$ resp. $L^2(E)$) as in the previous subsection to

$$\begin{aligned} \widehat{\eta}(\widehat{\mathcal{T}} \setminus \mathcal{T}) - \widetilde{\eta}(\widehat{\mathcal{T}} \setminus \mathcal{T}) &\leq \sum_{T \in \widehat{\mathcal{T}} \setminus \mathcal{T}} |T|^2 \|\widehat{\lambda}_h \widehat{u}_h - \lambda_h u_h - \Delta^2 \widehat{e}\|_{L^2(T)}^2 \\ &+ \sum_{T \in \widehat{\mathcal{T}} \setminus \mathcal{T}} |T|^{1/2} \sum_{E \in \widehat{\mathcal{E}}(T) \setminus \widehat{\mathcal{E}}(\Omega)} \|\partial_{\nu\nu}^2 \widehat{e}\|_E^2 + \sum_{T \in \widehat{\mathcal{T}} \setminus \mathcal{T}} |T|^{3/2} \sum_{E \in \widehat{\mathcal{E}}(T) \setminus \widehat{\mathcal{E}}(\Omega)} \|\partial_\nu \Delta \widehat{e}\|_E^2. \end{aligned}$$

The summands in the upper bound are identical to the situation in the previous subsection and the same argumentation applied on the fine level for $\widehat{\mathcal{T}} \setminus \mathcal{T}$ leads to

$$(29) \quad \widehat{\eta}(\widehat{\mathcal{T}} \setminus \mathcal{T}) \leq \widetilde{\eta}(\widehat{\mathcal{T}} \setminus \mathcal{T}) + \Lambda_2 \delta(\mathcal{T}, \widetilde{\mathcal{T}}).$$

The proof of the remaining reduction property $\widetilde{\eta}(\widehat{\mathcal{T}} \setminus \mathcal{T}) \leq 2^{-1/4} \eta(\mathcal{T} \setminus \widehat{\mathcal{T}})$ rewrites the sum over all fine but not coarse triangles $T \in \widehat{\mathcal{T}} \setminus \mathcal{T}$ as a double sum over all coarse but not fine triangles $K \in \mathcal{T} \setminus \widehat{\mathcal{T}}$ and its children in $\widehat{\mathcal{T}}(K) := \{T \in \widehat{\mathcal{T}} : T \subset K\}$. The point is that, for each $K \in \mathcal{T} \setminus \widehat{\mathcal{T}}$, a triangle $T \in \widehat{\mathcal{T}}(K)$ has been obtained by bisection of K at least once so that $|T| \leq |K|/2$ implies

$$\begin{aligned} \sum_{T \in \widehat{\mathcal{T}}(K)} \widetilde{\eta}^2(T) &\leq 2^{-2} |K|^2 \sum_{T \in \widehat{\mathcal{T}}(K)} \|\lambda_h u_h - \Delta^2 u_h\|_{L^2(T)}^2 \\ &+ 2^{-1/2} |K|^{1/2} \sum_{T \in \widehat{\mathcal{T}}(K)} \left(\sum_{E \in \mathcal{E}(T) \setminus \widehat{\mathcal{E}}(\Omega)} \|[\partial_{\nu\nu}^2 u_h]_E\|_{L^2(E)}^2 + 2^{-1} |K| \sum_{E \in \mathcal{E}(T) \setminus \widehat{\mathcal{E}}(\Omega)} \|[\partial_\nu \Delta u_h]_E\|_{L^2(E)}^2 \right). \end{aligned}$$

The sums over $T \in \widehat{\mathcal{T}}(K)$ combine directly in $\sum_{T \in \widehat{\mathcal{T}}(K)} \|\lambda_h u_h - \Delta^2 u_h\|_{L^2(T)}^2 = \|\lambda_h u_h - \Delta^2 u_h\|_{L^2(K)}^2$, while the jumps with respect to the fine geometry vanish for interior edges $\widehat{E} \in \widehat{\mathcal{E}}$ with $\widehat{E} \not\subset \partial K$ for u_h is a polynomial in K . Indeed, the non-zero summands for $\widehat{E} \in \mathcal{E}(T)$, $T \in \widehat{\mathcal{T}}(K)$, belong to the boundary $\widehat{E} \subset \partial K$ and sum up to the full L^2 norms along the coarse edges E of K . This explains

$$\begin{aligned} \sum_{T \in \widehat{\mathcal{T}}(K)} \sum_{E \in \mathcal{E}(T) \setminus \widehat{\mathcal{E}}(\Omega)} \|[\partial_{\nu\nu}^2 u_h]_E\|_{L^2(E)}^2 &= \|[\partial_{\nu\nu}^2 u_h]_E\|_{L^2(\partial K \setminus \Omega)}^2, \\ \sum_{T \in \widehat{\mathcal{T}}(K)} \sum_{E \in \mathcal{E}(T) \setminus \widehat{\mathcal{E}}(\Omega)} \|[\partial_\nu \Delta u_h]_E\|_{L^2(E)}^2 &= \|[\partial_\nu \Delta u_h]_E\|_{L^2(\partial K \setminus \Omega)}^2. \end{aligned}$$

The combination of the above estimates reveals (with the sum convention) that

$$\widehat{\eta}^2(\widehat{\mathcal{T}} \setminus \mathcal{T}) = \sum_{T \in \widehat{\mathcal{T}}(K)} \widetilde{\eta}^2(T) \leq 2^{-1/2} \eta^2(K) \quad \text{for } K \in \mathcal{T} \setminus \widehat{\mathcal{T}}.$$

This and (29) conclude the proof of (A2). \square

3.4. Proof of discrete reliability (A3). This subsection provides the discrete reliability in the 2-level notation of Subsection 2.4: Given $\mathcal{T} \in \mathbb{T}(\delta_3)$ with $\delta_3 \leq \delta_2$ as in Lemma 2.1 and 2.2. In fact, those preliminaries form the key arguments for

$$(A3) \quad \delta(\mathcal{T}, \widehat{\mathcal{T}}) = \|\widehat{e}\| \leq \Lambda_3 \eta(\mathcal{T} \setminus \widehat{\mathcal{T}}).$$

The proof of (A3) is finalized by the known arguments on [CH21] for the associated source problem with $f := \lambda_h u_h \in L^2(\Omega)$. In fact, Lemma 2.2 provides

$$(1 - \kappa) \|\widehat{e}\|^2 \leq \text{Res}(\widehat{e}) = \int_{\Omega} f \widehat{e} \, dx - a(u_h, \widehat{e})$$

and the latter residual is already considered in [CH21, Thm. 4]. With an identical proof, based on a discrete quasi-interpolation operator [CH21, Thm. 2] for $p = 5$ and further nowadays standard arguments in explicit residual-based a posteriori error control, that former result reveals

$$\int_{\Omega} f \widehat{e} \, dx - a(u_h, \widehat{e}) \leq \Lambda'_3 \|\widehat{e}\| \eta(\mathcal{T} \setminus \widehat{\mathcal{T}}).$$

The universal constant Λ'_3 (called Λ_3 in [CH21, Grä22]) depends on the polynomial degree of the Argyris finite element scheme and the shape regularity in \mathbb{T} ; Λ'_3 is independent of the discrete or continuous eigenvalues (i.e. independent of j fixed in the 2-level notation) and independent of any smallness assumption (i.e. independent of δ_3). This concludes the proof of (A3) with $\Lambda_3 := \Lambda'_3 / (1 - \kappa)$ for $p = 5$. The generalisation of [CH21, Thm. 2] for $p \geq 6$ is possible with the techniques of [CH21]. \square

3.5. Proof of quasi-orthogonality (A4). This is in fact an orthogonality based on the nestedness of the discrete spaces $V(\mathcal{T}_\ell) \subset V(\mathcal{T}_{\ell+1})$ already utilized in Lemma 2.1 and 2.2. The estimate $(1 - \kappa) \|\widehat{e}\|^2 \leq \lambda_h - \widehat{\lambda}_h$ of Lemma 2.2.a translates for $\mathcal{T} := \mathcal{T}_\ell$ and $\widehat{\mathcal{T}} := \mathcal{T}_{\ell+1}$ into

$$(1 - \kappa) \delta^2(\mathcal{T}_\ell, \mathcal{T}_{\ell+1}) \leq \lambda_\ell - \lambda_{\ell+1}$$

in terms of the output of the adaptive algorithm. For any $\ell, m \in \mathbb{N}_0$, this implies a telescoping sum

$$(1 - \kappa) \sum_{k=\ell}^{\ell+m} \delta^2(\mathcal{T}_k, \mathcal{T}_{k+1}) \leq \lambda_\ell - \lambda_{\ell+m+1}.$$

Lemma 2.2.a and (A3) for $\mathcal{T} := \mathcal{T}_\ell$ and $\widehat{\mathcal{T}} := \mathcal{T}_{\ell+m+1}$ provide

$$\lambda_\ell - \lambda_{\ell+m+1} \leq \delta^2(\mathcal{T}_\ell, \mathcal{T}_{\ell+m+1}) \leq \Lambda_3^2 \eta^2(\mathcal{T}_\ell).$$

The combination of the last two displayed estimates leads to $\Lambda_4 := \Lambda_3/(1 - \kappa)$ in

$$(A4) \quad \sum_{k=\ell}^{\ell+m} \delta^2(\mathcal{T}_k, \mathcal{T}_{k+1}) \leq \Lambda_4 \eta^2(\mathcal{T}_\ell) \quad \text{for all } \ell, m \in \mathbb{N}_0. \quad \square$$

3.6. Proof of optimal rates. This paper has established (A1)–(A3) for any triangulation $\mathcal{T} \in \mathbb{T}(\delta_2)$ and its refinement $\mathcal{T} \in \mathbb{T}(\mathcal{T})$ and (A4) for the outcome of AFEM provided $\mathcal{T}_0 \in \mathbb{T}(\delta_2)$. It is well established, that those properties imply optimality in the sense of (4) and conclude the proof of Theorem 1.1. This is proven explicitly in [CFPP14, CR17] and also follows with arguments from [CKNS08, Ste08]. \square

4. NUMERICAL RESULTS

This section provides striking numerical evidence of the optimal convergence rates for the proposed hierarchical adaptive Argyris FEM and thereby displays high-precision reference eigenvalues.

4.1. Comments on the implementation. Analytic exact eigenvalues are *not* available for basic geometries including the square domain in Subsection 4.2. The rapid convergence of the high-order Argyris AFEM results in a new state-of-the-art method for the computation of reference eigenvalues at the expense of a large condition number of the algebraic eigenvalue problem. Our realisation of the Argyris AFEM described in [Grä22] therefore utilizes multi-precision arithmetic [Zha23]. We evaluate integrals with an exact quadrature rule and expect all displayed digits in this section to be significant. An implicitly restarted Arnoldi method for the algebraic eigenvalue problem $Ax = \lambda Bx$ with mass matrix B and stiffness matrix A using the shift-and-invert strategy [Sco82, GLS94] solves the shifted problem $(A - \sigma B)^{-1} Bx = \alpha x$ with eigenvalues $\lambda = \sigma + \alpha^{-1}$ for the shift $\sigma \geq 0$ with $\sigma = 0$ if not stated otherwise. We note that the efficient solution of the algebraic eigenvalue problem, e.g., by preconditioned multilevel schemes available for the source problem [BZ95, AP21, CH21, Grä22], is left for future research.

This section considers clamped boundary conditions ($u|_{\Gamma_C} \equiv 0 \equiv u|_{\Gamma_C}$) on a closed part $\Gamma_C \subset \partial\Omega$ and simply-supported boundary conditions ($u|_{\Gamma_S} \equiv 0$) on a relatively open part $\Gamma_S \subset \partial\Omega$ of the boundary. The hierarchical Argyris AFEM for the mixed boundary conditions is discussed in [Grä22] and leads to the modified error estimator $\eta = \left(\sum_{T \in \mathcal{T}} \eta^2(T) \right)^{1/2}$ with the local contributions

$$\begin{aligned} \eta^2(T) &= |T|^2 \|\lambda_h u_h - \Delta^2 u_h\|_{L^2(T)}^2 \\ &\quad + |T|^{1/2} \|\partial_{\nu\nu}^2 u_h\|_{L^2(\partial T \setminus \Gamma_C)}^2 + |T|^{3/2} \|\partial_{\tau\tau\nu}^3 u_h + \partial_\nu \Delta u_h\|_{L^2(\partial T \setminus (\Gamma_C \cup \Gamma_S))}^2. \end{aligned}$$

The differences of this estimator to (3) are the modified jumps on the free boundary $\Gamma_F := \partial\Omega \setminus (\Gamma_C \cup \Gamma_S)$. On interior edges $E \in \mathcal{E}(\Omega)$, $[\partial_{\tau\tau\nu}^3 u_h]_E$ vanishes by the C^1 continuity of the discrete solution $u_h \in V(\mathcal{T})$ and the jumps coincide with those in (3). The optimal convergence rates from Section 3 generalizes to the mixed boundary conditions of this problem. The benchmarks compare AFEM (with $\theta = 0.5$ unless stated otherwise) and uniform red-refinement, where each triangle is divided into four congruent triangles by joining the edge midpoints; ndof abbreviates the number of degrees of freedom.

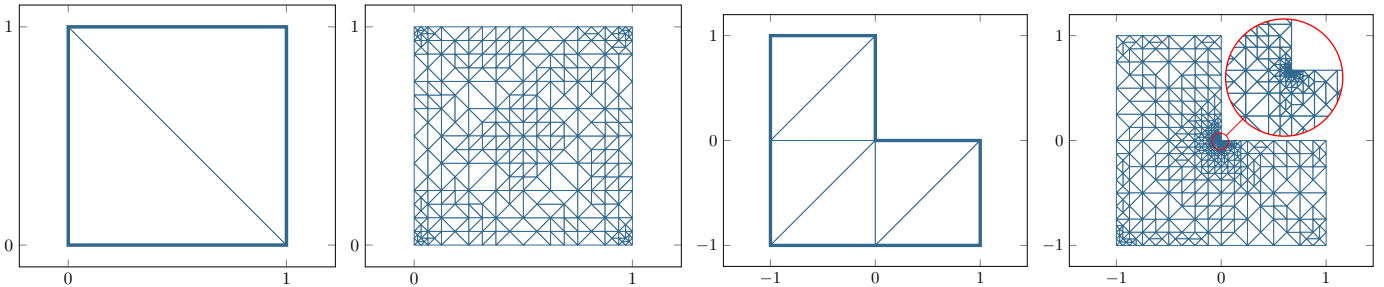


FIGURE 2. Initial and adaptive triangulations of the unit square and the L-shaped domain

Square	
λ_1	1294.9339795917128081703026479743085522513148
$\lambda_2 = \lambda_3$	5386.6565607779451709440883164319500534323747
λ_4	11710.811238205718716479524026744165110548790
λ_5	17313.499721776700784267277477409032730611369
λ_6	17478.106551478646880691169158961070602062916
$\lambda_7 = \lambda_8$	27225.134042723468407942851261240075600133838
$\lambda_9 = \lambda_{10}$	44319.444997239644605551889845792194008818266

TABLE 1. First ten eigenvalues of the unit square

4.2. High-precision eigenvalues on the square. The approximation of the principal eigenvalue on the unit square $\Omega = (0, 1)^2$ results in the reduced empirical convergence rate 2.5 in terms of ndof under uniform mesh refinement shown in Figure 3.

AFEM for $\theta = 0.5$ and $p = 13$ computes the reference values in Table 1 on an adaptive mesh with 2×10^6 ndofs in between 70–85 levels. The multiple eigenvalues $\lambda_2 = \lambda_3, \lambda_7 = \lambda_8$, and $\lambda_9 = \lambda_{10}$ lead to numerical instability of the Arnoldi method if no shift $\sigma = 0$ was applied. In this case, only up to 32 significant digits of λ_3 to λ_{10} , independent of the precision in the computations, could be obtained. The remedy with a shift leads to the reference values in Table 1: the shift σ therein is the integral part of the respective eigenvalue. Figure 3 displays the optimal convergence rates of the Argyris AFEM for different polynomial degrees p that are guaranteed by Theorem 1.1 also for a modification of AFEM with $\theta = 0.1$ and a successive p -increase. In the successive p -increase, the AFEM remains as described in Figure 1 but for variable polynomial degrees: For $\ell = 0$, let $p = 5$ and increase $p := p + 1$ after additional $2p$ levels, i.e., $p = 5$ for $\ell = 0, \dots, 9$, $p = 6$ for $\ell = 10, \dots, 21$, $p = 7$ for $\ell = 22, \dots, 35$, etc. The latter strategy offers a highly efficient alternative with super-algebraic convergence rates at comparable computational costs. The horizontal lines in Figure 3 indicate the known eigenvalue inclusions from [Wie97] and the high-precision reference value from [BT99].

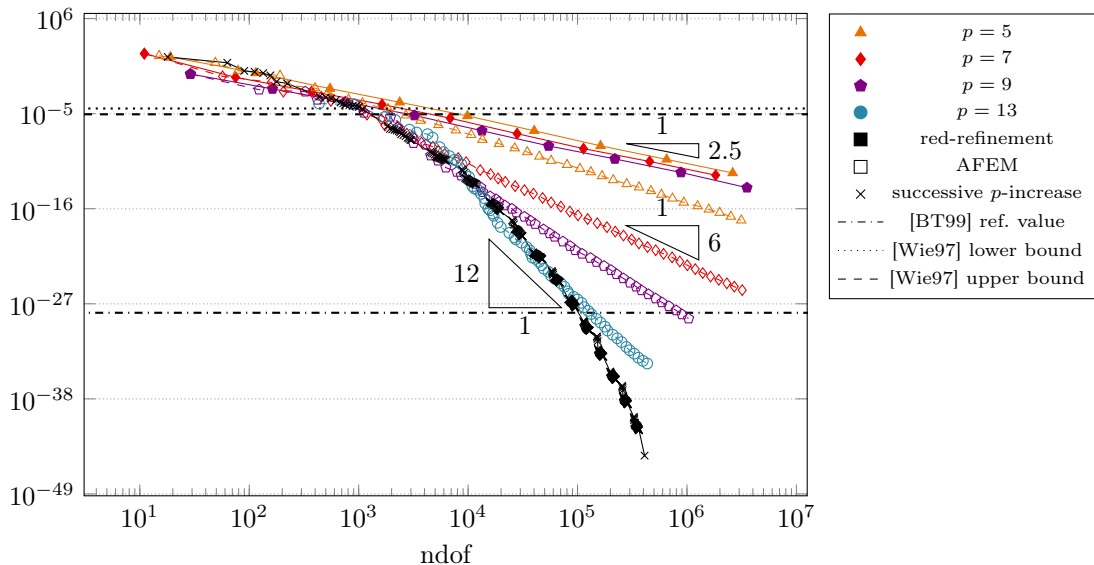


FIGURE 3. Convergence history plot of AFEM (hollow) and uniform-red refinement (filled) towards the principal eigenvalue λ_1 of the unit square for different p and a successive p -increase

4.3. L-shaped domain. The L-shaped domain $\Omega := (-1, 1)^2 \setminus [0, 1)^2$ with initial triangulation in Figure 2 has an index of elliptic regularity $\sigma_{\text{reg}} = 0.54$ [Gri92]. Figure 4 displays the expected suboptimal convergence rate $\sigma_{\text{reg}} = 0.54$ (in terms of the degrees of freedom) under uniform refinement for λ_1 and λ_{10} . The adaptive algorithm refines towards the singularity at the origin $(0, 0)$ as shown in Figure 2 for $p = 5$ and recovers optimal convergence rates $p - 1$ asymptotically as predicted by Theorem 1.1 for a sufficiently small maximal mesh-size of the initial triangulation.

L-shape	
λ_1	418.9752928519954616775618775449403
λ_2	690.9065117037020521173375432095840
λ_3	931.5792655819233500496763905727078
λ_4	1634.533781725410909450276640848249
λ_5	2090.839376830117972780944169183919
λ_6	3350.410627882138361796676879507818
λ_7	3720.925878799246215492176662379798
λ_8	4485.620042035762239796922517307530
λ_9	4560.432156327978825966680488256231
λ_{10}	5738.403842705743348891002113406246

TABLE 2. Reference values for the L-shaped domain

AFEM recovers optimal asymptotic rates already for very coarse initial triangulations in Figure 4, but exhibits a pre-asymptotic behaviour with reduced convergence rates on coarse meshes. Initial red-refinements offer a cheap way to reduce the computational time in the pre-asymptotic regime of sub-optimal convergence which length depends on the polynomial degree p and the approximated eigenvalue. Figure 4 compares AFEM for $\theta = 0.5$ and $p = 5$ applied to $n = 0, 1, 2, 3$ (displayed with differently shaped markers) initial red-refinements of the initial triangulation from Figure 2. Already two initial red-refinements remove the pre-asymptotic regime almost completely, whereas an even higher number of initial red-refinements lead to a superconvergence behaviour of AFEM with many small increments of ndof until the convergence graphs meet and exhibit the same convergence error.

Table 2 provides reference values of the first ten eigenvalues on the L-shaped domain.

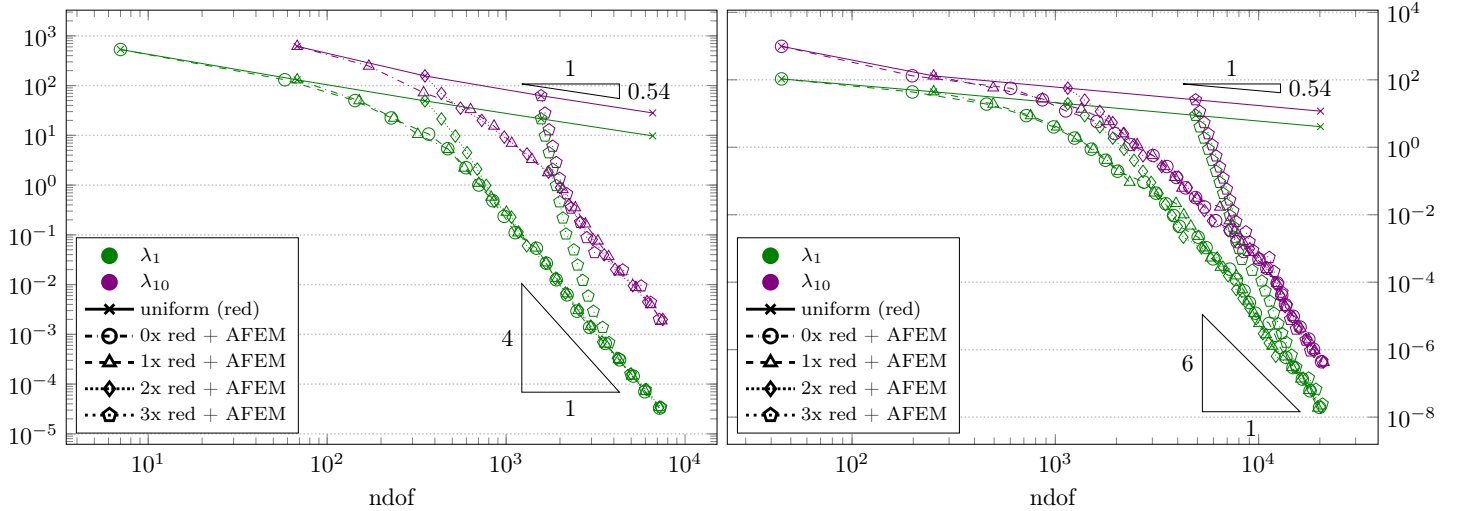


FIGURE 4. Convergence history plot of λ_1 and λ_{10} from AFEM ($p = 5$ left and $p = 7$ right) with $n = 0, 1, 2, 3$ -times red-refinement of \mathcal{T}_0 from Figure 2 as initial triangulation

4.4. Isospectral domains. The spectrum of the Laplacian for different domains can coincide [GWW92, Bus86, BCDS94, Kac66]; Figure 6 displays the initial triangulation of two Laplace-isospectral domains. Our computations provide numerical evidence that these domains are also isospectral for the biharmonic operator under simply-supported boundary conditions ($u = 0$ on $\partial\Omega$ in $V = H^2(\Omega) \cap H_0^1(\Omega)$), cf. Remark 4.1 for an explanation. Table 3 provides reference values of the biharmonic operator for the isospectral domains of Figure 6 under simply-supported boundary conditions and verifies that these domains are *not* isospectral under clamped boundary conditions ($u = 0 = \partial_\nu u$ on $\partial\Omega$) of (1). The ninth eigenfunction $u_9(x, y) = \cos(\pi x/2) \sin(\pi y) - \cos(\pi y/2) \sin(\pi x) \in C^\infty(\Omega) \cap H_0^1(\Omega)$ of the Dirichlet-Laplacian on both domains in Figure 6 is special [Dri97]. Restricted to each right-isosceles triangle $T \in \mathcal{T}$ in Figure 6, $u_9|_T$ is the first eigenmode of the Laplacian (on that triangle) described in [DPCD10] with eigenvalue $5\pi^2/4$. Since $u_9 \in H^2(\Omega) \cap H_0^1(\Omega)$, it is also an eigenfunction of the biharmonic operator with simply-supported boundary conditions for the eigenvalue $(5\pi^2/4)^2 = \lambda_9$ in Table 3.

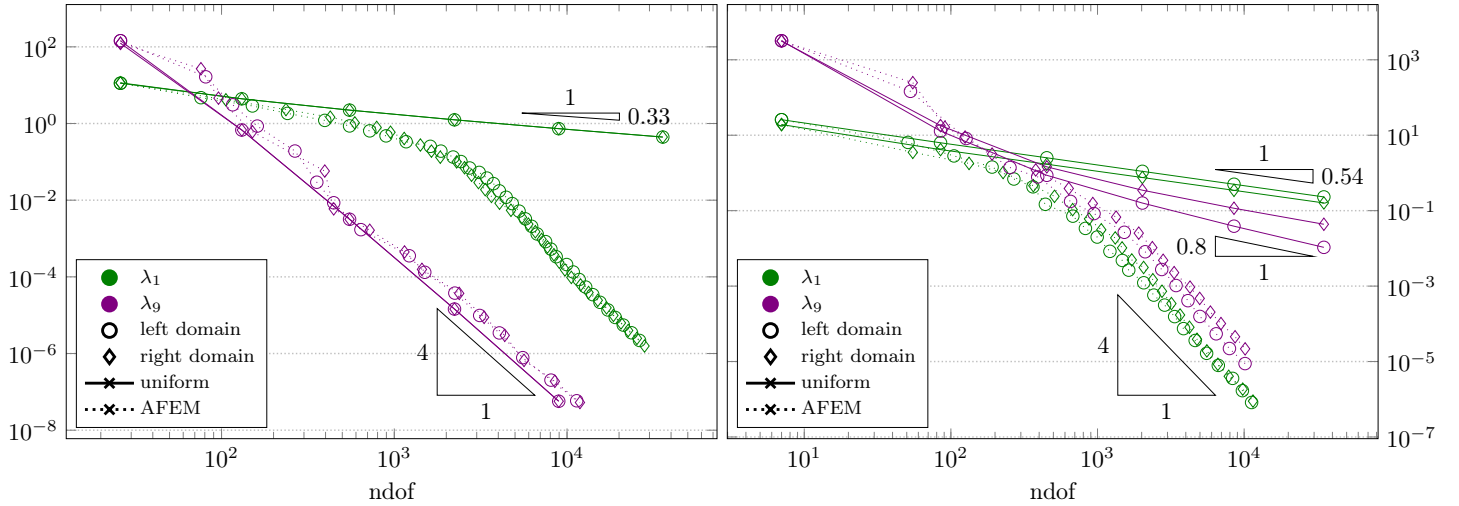


FIGURE 5. Convergence history plot of λ_1 and λ_9 on the two domains of Figure 6 with simply-supported (left) and clamped boundary conditions (right)

The smoothness of u_9 leads in Figure 5 to optimal convergence rates under both uniform and adaptive refinement for $p = 5$. This is in contrast to the principal eigenvalue of the biharmonic under simply-supported boundary conditions with a small convergence of rate 0.33 under uniform refinement. No localisation of eigenfunctions over the congruent triangles of Figure 6 similar to that of u_9 has been observed for the biharmonic operator with clamped boundary conditions. AFEM recovers optimal convergence rates in all cases. The observed convergence rate 0.8 (on the right) for the ninth eigenfunction under uniform refinement over the displayed computational domain may be preasymptotic.

Remark 4.1 (Isospectrality for simply-supported boundary conditions). *The proof of isospectrality for two domains Ω_1 and Ω_2 by the transplantation technique from Buser [Bus86] for the Laplace operator explicitly constructs a map $\Phi : H_0^1(\Omega_1) \rightarrow H_0^1(\Omega_2)$ that transforms an eigenfunction $u_1(\lambda)$ of Ω_1 to an eigenfunction $u_2(\lambda)$ with the same eigenvalue λ on the second domain Ω_2 . In short, that technique relies on triangulations \mathcal{T}_1 and \mathcal{T}_2 of Ω_1 and Ω_2 into congruent triangles as in Figure 6. The idea is then to locally construct an eigenfunction $u_2(\lambda)|_K$ on a triangle $K \in \mathcal{T}_2$ in Ω_2 for the same eigenvalue λ as a linear combination of re-transformed $\{u_1(\lambda)|_T\}_{T \in \mathcal{T}_1}$. Then $u_2 \in H_0^1(\Omega)$ becomes an eigenfunction on Ω_2 with eigenvalue λ . A list of domain pairs that allow such a design is studied in [BCDS94]. A careful investigation of the continuity and boundary conditions of the transplanted function verifies that this technique also applies to the biharmonic operator under simply-supported boundary conditions but fails for the clamped boundary conditions. This justifies the experimentally verified isospectrality only for simply-supported boundary conditions, but fails for clamped boundary conditions.*

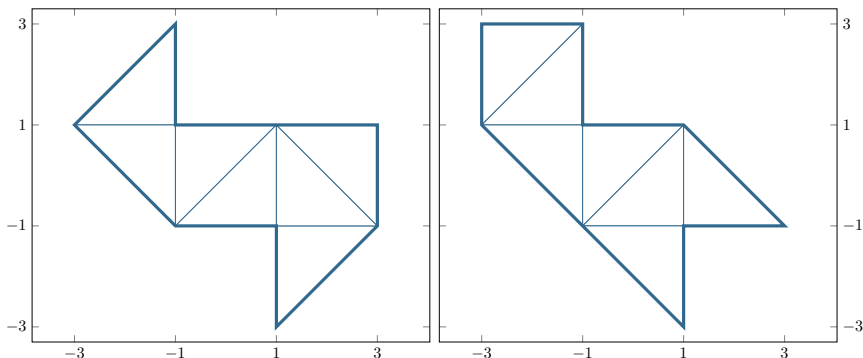


FIGURE 6. Two isospectral domains for the Laplacian or the biharmonic operator under simply-supported boundary conditions

	simply-supported (both domains)	clamped (left domain)	clamped (right domain)
λ_1	10.36402107986949540721	28.0586863865423000549087398	25.01410502064436259175268775
λ_2	16.402184923407268356740	42.80755796191819473005366012	50.67098031228146895086815044
λ_3	36.28192141809921686643	73.51576421441210956574548706	72.0887124830690440717331005
λ_4	47.33781364226172710396	109.355356090831716811598988	101.50786786148196218598065170
λ_5	61.23040947172451684072	123.8961882657907045115913099	119.568610048818932875544158
λ_6	90.01373420512098390986	151.830513099492311414264541	162.5851723649249044594031075
λ_7	119.052506025401956876870	227.038626156347910723847312	217.9878528191822288137668706
λ_8	135.11181644660087949787	251.63057739930330617446625802	263.6684022735138072395955186
λ_9	152.2017047406288081819380	290.252435400071762741097143187	297.5045897085804999794427456
λ_{10}	187.12311642208418946283	311.16810084585353295577573668	315.5017873309864911264409052

TABLE 3. Eigenvalues of the biharmonic operator for the two domains in Figure 6 under simply-supported (left) and under clamped boundary conditions (middle and right)

4.5. Experiments on the rectangle with hole. This benchmark considers the domain $\Omega := R \setminus [0, 1]^2$ displayed in Figure 7 with free boundary conditions on the outer boundary $\Gamma_F = \partial R$ of the rectangle $R = (-1, 3) \times (-1, 4)$ and clamped boundary conditions on the interior boundary $\Gamma_C = \partial[0, 1]^2$. The abstract setting of Section 2 applies for this problem with mixed boundary conditions in the space of admissible functions $V := \{v \in H_0^2(\Omega) : v|_{\Gamma_C} = 0 = \partial_\nu v|_{\Gamma_C}\}$.

Undisplayed computations reveal the empirical convergence rate 0.54 (in terms of ndof) for the approximation of the principal eigenvalue under uniform mesh-refinement. This suggests that the corresponding eigenfunction has the same regularity as for the L-shaped domain of Subsection 4.3. AFEM for the initial triangulation of Figure 7 locally refines towards the four reentering corners with different intensity (depending on the approximated eigenvalue) and recovers optimal convergence rates in Figure 8 for $p = 5$ already on coarse triangulations. A smaller bulk parameter θ results in a lower error on fine meshes for the approximation of three displayed eigenvalues, at the cost of an increased number of iterations in the AFEM loop. However, the asymptotic improvement of $\theta < 0.5$ over $\theta = 0.5$ appears negligible. If the discrete spectrum is not resolved sufficiently accurate, a small value $\theta = 0.1$ for the approximation of λ_{10} in Figure 8 even enlarges the preasymptotic regime. One uniform red-refinement (undisplayed) of the initial mesh removes the observed preasymptotic behaviour and leads to the guaranteed optimal rates from the first iteration with $\text{ndof}=786$.

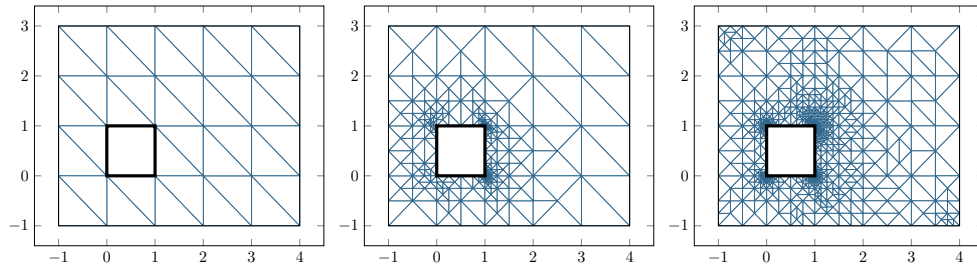


FIGURE 7. Initial triangulation (left) and adaptive refinements with $|\mathcal{T}| = 572$ (middle) and $|\mathcal{T}| = 2528$ (right) for the principal eigenvalue and $p = 5$ in Subsection 4.5

λ_1	0.10698498562334817102814013
λ_2	0.35605676603875088420438615
λ_3	0.94524070807442103593431671
λ_4	2.53208704546115218637535529
λ_5	3.99930885285784387075239865
λ_6	5.57646932761755697998226709
λ_7	6.43857726128711796898224149
λ_8	9.13840065843740557418337614
λ_9	16.4479467402360010159306274
λ_{10}	17.4245866515989760773466203

TABLE 4. First ten eigenvalues for the rectangle with a hole

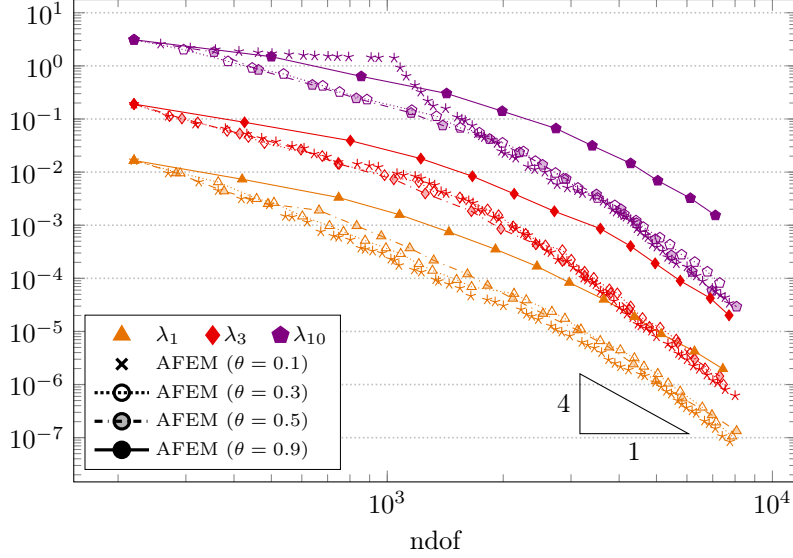


FIGURE 8. Convergence history plot of AFEM with different bulk parameters θ for some eigenvalues in Subsection 4.5

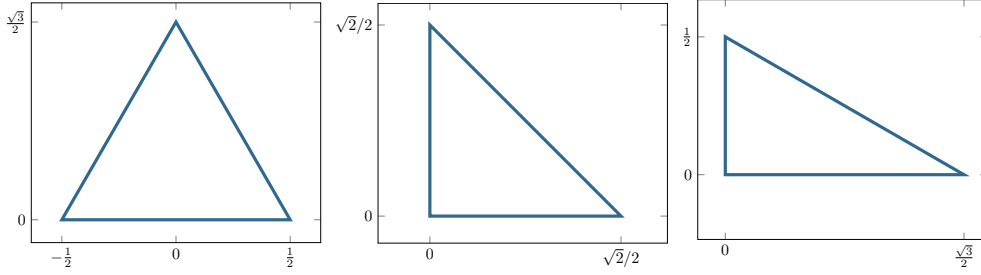


FIGURE 9. Equilateral, Right-isoceles, and 90-60-30 triangle scaled to $h_T = 1$

4.6. Constants related to eigenvalues on triangles. This benchmark reports on some eigenvalues related to constants in standard interpolation estimates for the equilateral triangle, right-isoceles triangle, and the right triangle with angles 90-60-30 depicted in Figure 4.6. Let $T \subset \mathbb{R}^2$ be a triangle and $V \subset H^2(T)$ such that $V \cap P_1(T) = \{0\}$. A scaling argument verifies that the best-possible constants C_0 and C_1 in

$$(30) \quad \|v\|_{L^2(T)} \leq C_0 h_T^2 \|D^2 v\|_{L^2(T)} \quad \text{and} \quad \|\nabla v\|_{L^2(T)} \leq C_1 h_T \|D^2 v\|_{L^2(T)} \quad \text{for all } v \in V$$

exclusively depend on the shape of the triangle T . By the Rayleigh-Ritz (or min-max) principle, $\lambda_{\min} = (C_s h_T^s)^{-2}$ is the minimal eigenvalue of the eigenvalue problem

$$(31) \quad (D^2 u, D^2 v)_{L^2(T)} = \lambda b_s(u, v)_{L^2(T)} \quad \text{for all } v \in V$$

with $b_0(\bullet, \bullet) = b(\bullet, \bullet) = (\bullet, \bullet)_{L^2(T)}$ for $s = 0$ as in Section 2 and $b_1(\bullet, \bullet) = (\nabla \bullet, \nabla \bullet)_{L^2(T)}$ for $s = 1$ as in plate buckling. This subsection considers (30)–(31) for the four spaces, $V_C := H_0^2(T)$ for clamped boundary conditions, $V_S := H^2(T) \cap H_0^1(T)$ for simply-supported boundary conditions, and

$$V_V := \{f \in H^2(T) : f(z) = 0 \text{ for all } z \in V(T)\},$$

$$V_M := \{f \in H^2(T) : f(z) = 0 \text{ for all } z \in V(T) \text{ and } \int_E f \, ds = 0 \text{ for all } E \in \mathcal{E}(T)\}.$$

The spaces V_V and V_M encode boundary conditions related to the P_1 interpolation $I_V : H^2(T) \rightarrow P_1(T)$ [BS08] and the Morley interpolation $I_M : H^2(T) \rightarrow P_2(T)$ [Mor68] over the triangle T .

For the three triangular shapes with $h_T = 1$ from Figure 4.6, Table 5 displays the principal eigenvalues $\lambda_{\min} = C_s^{-2}$ of (31) for $s \in \{0, 1\}$ and the four spaces V_X with $X \in \{C, S, V, M\}$. In particular, for the Morley-type boundary conditions in $V = V_M$, the constants in the Morley interpolation estimate read

$$C_0 = 0.07350005475651561, \quad C_1 = 0.1743250725741249$$

s	X	equilateral	right-isosceles	90-60-30
0	C	9804.9449874764568054397360472302	35185.638471713425529039119075	55407.231456202639937488311240
	S	2770.74747830051377028096946314538	9740.9091034002437236440332688705	15085.180715191686082640833743
	V	72.942664620393689247350334919683	142.9905816658059570843982031023	120.61629780957915519675157481
	M	185.10778102243532486304991536227	492.33162470634854919442608899	391.7946452226036199316742042
1	C	146.412905109344790007913155148663	279.14825470003949590687643840	352.12132391711858946305008173
	S	52.6378901391432459671172853326728	98.696044010893586188344909998761	122.82174365800090725660699910
	V	9.86394388190996483130098955949938	8.37347027272868454327196355771	8.5380950929242319268917035189
	M	32.906393793581628348514192294762	36.63077785104390025356999314735	33.45210121650411459840950230

TABLE 5. Principal eigenvalues for different boundary conditions in the space V_X with $X \in \{C, S, V, M\}$ on the equilateral, right-isosceles, and 90-60-30 triangle of Figure 4.6

for the equilateral triangle and for the right-isosceles triangle

$$C_0 = 0.045068295511191264, \quad C_1 = 0.16522544473105152.$$

Those improve the numerical values in [LSL19] where it is suggested that the equilateral triangle leads to the maximal value C_0 amongst all triangles.

Remark 4.2. Note that the constants C_0, C_1 for $V = V_M$ coincide with the best-possible constants in the local Morley interpolation error estimate, i.e., C_0, C_1 from (30) for $V = V_M$ are best-possible in

$$\|(1 - I_M)v\|_{L^2(T)} \leq C_0 h_T^2 \|D^2 v\|_{L^2(T)}, \quad \|\nabla(1 - I_M)v\|_{L^2(T)} \leq C_1 h_T \|D^2 v\|_{L^2(T)} \quad \text{for all } v \in H^2(T).$$

This follows from $V_M = (1 - I_M)H^2(T) \subset H^2(T)$, $I_M V_M = \{0\}$, and $\|D^2(1 - I_M)\bullet\|_{L^2(T)} \leq \|D^2\bullet\|_{L^2(T)}$; see [HSX12, CGH14, Gal15] for details on the Morley interpolation I_M .

4.7. Conclusions. The few methods for high-precision reference values in the literature, e.g., [BT99], highly depend on structural properties of the domain and do not immediately extend to general domains. The high-order Argyris FEM demands an adaptive algorithm and the presented hierarchical Argyris AFEM offers efficient computations of accurate eigenvalues on general polygonal domains.

The restriction to sufficiently fine initial triangulations and a small bulk parameter θ for optimal asymptotic convergence rates from Theorem 1.1 is *not* visible in the examples. A coarse initial triangulation or a large bulk parameter θ close to 1 increase the preasymptotic regime. Our overall numerical experience supports our impression that $\theta = 0.5$ is a good choice. After a small number of initial red-refinements to obtain \mathcal{T}_0 AFEM enters the asymptotical regime immediately.

While this paper focusses on simple eigenvalues, a generalisation of the theoretical result for multiple eigenvalues or eigenvalue clusters is possible with the cluster algorithm from [Gal14]. In all presented applications, however, the AFEM algorithm from Figure 1 suffices and converges optimally also towards multiple eigenvalues (e.g., for the square in Subsection 4.2) provided that the algebraic eigenvalue problem solve is sufficiently accurate.

REFERENCES

- [AFS68] J. H. Argyris, I. Fried, and D. W. Scharpf. The TUBA Family of Plate Elements for the Matrix Displacement Method. *Aeronaut. J.*, (692):701–709, 1968.
- [AP21] M. Ainsworth and C. Parker. Preconditioning high order H^2 conforming finite elements on triangles. *Numer. Math.*, (2):223–254, 2021.
- [BC17] S. C. Brenner and C. Carstensen. Finite Element Methods. In *Encyclopedia of Computational Mechanics Second Edition*, pages 1–47. John Wiley & Sons, Ltd, Chichester, UK, 2017.
- [BCDS94] P. Buser, J. Conway, P. Doyle, and K.-D. Semmler. Some planar isospectral domains. *Internat. Math. Res. Notices*, (9):391, 1994.
- [BDD04] P. Binev, W. Dahmen, and R. DeVore. Adaptive Finite Element Methods with convergence rates. *Numer. Math.*, (2):219–268, 2004.
- [Bel68] K. Bell. *Analysis of Thin Plates in Bending Using Triangular Finite Elements*. Division of Structural Mechanics, Techn. University of Norway, 1968.
- [Bel69] K. Bell. A refined triangular plate bending finite element. *Int. J. Numer. Meth. Engng.*, (1):101–122, 1969.
- [BO91] I. Babuška and J. Osborn. Eigenvalue problems. In *Handbook of Numerical Analysis*, pages 641–787. Elsevier, 1991.
- [Bof10] D. Boffi. Finite element approximation of eigenvalue problems. *Acta Numerica*, pages 1–120, 2010.
- [Bos68] W. Bosshard. Ein neues, vollverträgliches endliches Element für Plattenbiegung. *Int. Ver. Für Brückenbau Hochbau Abh.*, (1), 1968.
- [Bra07] D. Braess. *Finite Elements: Theory, Fast Solvers, and Applications in Elasticity Theory*. Cambridge University Press, Cambridge, 3 edition, 2007.

- [Bre11] H. Brezis. *Functional Analysis, Sobolev Spaces and Partial Differential Equations*. Springer New York, New York, NY, 2011.
- [BS05] S. C. Brenner and L.-Y. Sung. C^0 interior penalty methods for fourth order elliptic boundary value problems on polygonal domains. *J Sci Comput*, (1-3):83–118, 2005.
- [BS08] S. C. Brenner and L. R. Scott. *The Mathematical Theory of Finite Element Methods*. Texts in Applied Mathematics. Springer New York, New York, NY, 2008.
- [BT99] P. E. Bjørstad and B. P. Tjøstheim. High Precision Solutions of Two Fourth Order Eigenvalue Problems. *Computing*, (2):97–107, 1999.
- [Bus86] P. Buser. Isospectral riemann surfaces. *Ann. Inst. Fourier*, (2):167–192, 1986.
- [BZ95] J. H. Bramble and X. Zhang. Multigrid methods for the biharmonic problem discretized by conforming C^1 finite elements on nonnested meshes. *Numerical Functional Analysis and Optimization*, (7-8):835–846, 1995.
- [CFPP14] C. Carstensen, M. Feischl, M. Page, and D. Praetorius. Axioms of adaptivity. *Comput. Math. Appl.*, (6):1195–1253, 2014.
- [CG11] C. Carstensen and J. Gedicke. An oscillation-free adaptive FEM for symmetric eigenvalue problems. *Numer. Math.*, (3):401–427, 2011.
- [CG24] C. Carstensen and B. Gräßle. [Manuscript in preparation]. 2024.
- [CGH14] C. Carstensen, D. Gallistl, and J. Hu. A discrete Helmholtz decomposition with Morley finite element functions and the optimality of adaptive finite element schemes. *Comput. Math. Appl.*, (12):2167–2181, 2014.
- [CH21] C. Carstensen and J. Hu. Hierarchical Argyris Finite Element Method for Adaptive and Multigrid Algorithms. *Comput. Methods Appl. Math.*, (3):529–556, 2021.
- [Cia02] P. G. Ciarlet. *The Finite Element Method for Elliptic Problems*. Classics in Applied Mathematics. Society for Industrial and Applied Mathematics, 2002.
- [CKNS08] J. Cascon, C. Kreuzer, R. Nochetto, and K. Siebert. Quasi-optimal convergence rate for an adaptive finite element method. *SIAM J. Numer. Anal.*, (5):2524–2550, 2008.
- [CR17] C. Carstensen and H. Rabus. Axioms of Adaptivity with Separate Marking for Data Resolution. *SIAM J. Numer. Anal.*, (6):2644–2665, 2017.
- [DPCD10] A. Damle, G. Peterson, J. Curry, and A. Dougherty. Understanding the eigenstructure of various triangles. *SIAM Undergrad. Res. Online*, 2010.
- [Dri97] T. A. Driscoll. Eigenmodes of Isospectral Drums. *SIAM Rev.*, (1):1–17, 1997.
- [EG17] A. Ern and J.-L. Guermond. Finite element quasi-interpolation and best approximation. *ESAIM: M2AN*, (4):1367–1385, 2017.
- [Gal14] D. Gallistl. *Adaptive Finite Element Computation of Eigenvalues*. PhD thesis, Humboldt-Universität zu Berlin, Mathematisch-Naturwissenschaftliche Fakultät. <https://edoc.hu-berlin.de/handle/18452/17654>, 2014.
- [Gal15] D. Gallistl. An optimal adaptive FEM for eigenvalue clusters. *Numer. Math.*, (3):467–496, 2015.
- [GLS94] R. G. Grimes, J. G. Lewis, and H. D. Simon. A Shifted Block Lanczos Algorithm for Solving Sparse Symmetric Generalized Eigenproblems. *SIAM J. Matrix Anal. & Appl.*, (1):228–272, 1994.
- [Grä22] B. Gräßle. Optimal multilevel adaptive FEM for the Argyris element. *Comput. Methods Appl. Mech. Eng.*, page 115352, 2022.
- [Gri85] P. Grisvard. *Elliptic Problems in Nonsmooth Domains*. Society for Industrial and Applied Mathematics, 1985.
- [Gri92] P. Grisvard. *Singularities in Boundary Value Problems*. Number 22 in Research Notes in Applied Mathematics. Masson, Paris, 1992.
- [GWW92] C. Gordon, D. L. Webb, and S. Wolpert. One cannot hear the shape of a drum. *Bull. Amer. Math. Soc.*, (1):134–138, 1992.
- [HSX12] J. Hu, Z. Shi, and J. Xu. Convergence and optimality of the adaptive Morley element method. *Numer. Math.*, (4):731–752, 2012.
- [Kac66] M. Kac. Can One Hear the Shape of a Drum? *The American Mathematical Monthly*, (4):1, 1966.
- [LSL19] S.-K. Liao, Y.-C. Shu, and X. Liu. Optimal estimation for the Fujino–Morley interpolation error constants. *Japan J. Indust. Appl. Math.*, (2):521–542, 2019.
- [Mor68] L. S. D. Morley. The triangular equilibrium element in the solution of plate bending problems. *Aeronaut. Q.*, (2):149–169, 1968.
- [Rud91] W. Rudin. *Functional Analysis*. International Series in Pure and Applied Mathematics. McGraw-Hill, New York, 2nd ed edition, 1991.
- [Sco82] D. S. Scott. The Advantages of Inverted Operators in Rayleigh–Ritz Approximations. *SIAM J. Sci. and Stat. Comput.*, (1):68–75, 1982.
- [SF73] G. Strang and G. J. Fix. *An Analysis of the Finite Element Method*. Prentice-Hall Series in Automatic Computation. Prentice-Hall, Englewood Cliffs, N.J, 1973.
- [Ste08] R. Stevenson. The completion of locally refined simplicial partitions created by bisection. *Math. Comp.*, (261):227–241, 2008.
- [Ver96] R. Verfürth. *A Review of a Posteriori Error Estimation and Adaptive Mesh-Refinement Techniques*. Wiley-Teubner Series, Advances in Numerical Mathematics. Wiley-Teubner, Chichester ; New York, 1996.
- [Vis68] W. Visser. *The Finite Element Method in Deformation and Heat Conduction Problems*. PhD thesis, Delft University of Technology, 1968.
- [Wie97] C. Wieters. Bounds for the N lowest eigenvalues of fourth-order boundary value problems. *Computing*, (1):29–41, 1997.
- [Wit66] D. Withum. *Berechnung von Platten Nach Dem Ritzschen Verfahren Mit Hilfe Dreieckförmiger Maschennetze*. Techn. Hochschule, Inst. f. Statik, 1966.
- [Yos95] K. Yosida. *Functional Analysis*. Classics in Mathematics. Springer Berlin Heidelberg, Berlin, Heidelberg, 1995.
- [Zei92] E. Zeidler. *Nonlinear Functional Analysis and Its Applications. 1: Fixed-point Theorems*. Springer, New York, softcover reprint of the hardcover 1st edition 1986, second corrected printing edition, 1992.
- [Zha23] D. K. Zhang. MultiFloats.jl. <https://github.com/dzhang314/MultiFloats.jl>, 2023.

(C. Carstensen, B. Gräßle) DEPARTMENT OF MATHEMATICS, HUMBOLDT-UNIVERSITÄT ZU BERLIN, 10117 BERLIN, GERMANY; cc@math.hu-berlin.de, graesslb@math.hu-berlin.de